

AD-A057 505

DAYTON UNIV OHIO RESEARCH INST

F/G 20/4

THE AEROELASTIC ANALYSIS OF A TWO-DIMENSIONAL AIRFOIL IN TRANSO--ETC(U)

DEC 77 D P RIZZETTA

F33615-76-C-3146

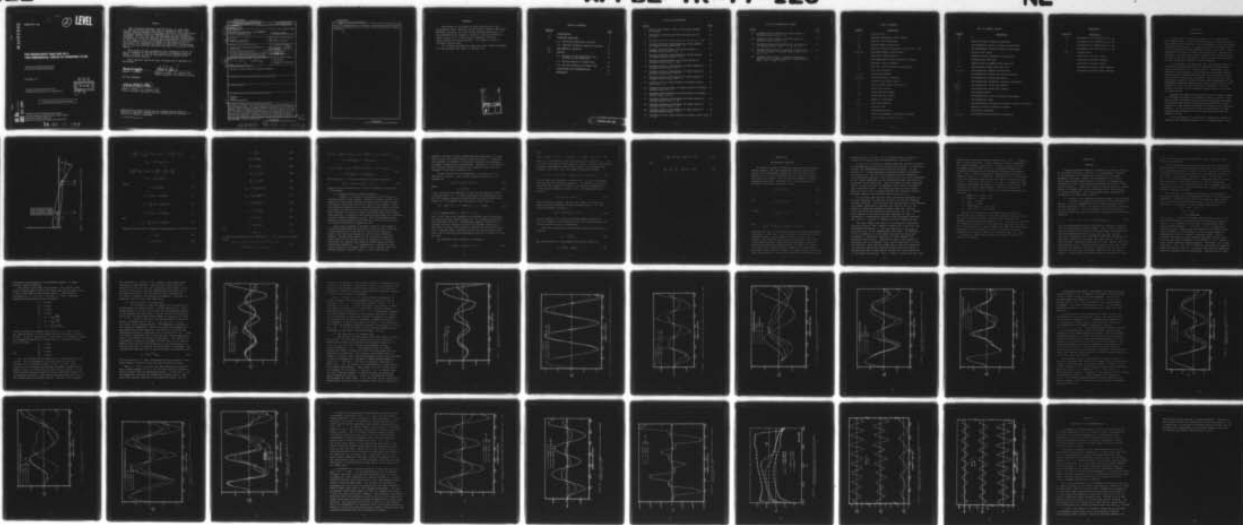
UNCLASSIFIED

AFFDL-TR-77-126

NL

| of |

AD
A057 505



END

DATE

FILMED

9-78

DDC

AD A057505

AFFDL-TR-77-126

2

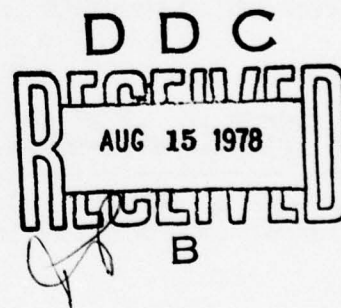
LEVEL II

THE AEROELASTIC ANALYSIS OF A TWO-DIMENSIONAL AIRFOIL IN TRANSONIC FLOW

*ANALYSIS & OPTIMIZATION BRANCH
STRUCTURAL MECHANICS DIVISION*

DECEMBER 1977

TECHNICAL REPORT AFFDL-TR-77-126
Final Report for Period July 1977 - September 1977



Approved for public release; distribution unlimited.

AD No. _____
DDC FILE COPY

AIR FORCE FLIGHT DYNAMICS LABORATORY
AIR FORCE WRIGHT AERONAUTICAL LABORATORIES
AIR FORCE SYSTEMS COMMAND
WRIGHT-PATTERSON AIR FORCE BASE, OHIO 45433

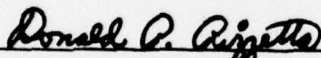
78 08 07 097

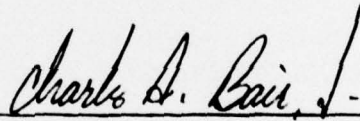
NOTICE

When Government drawings, specifications, or other data are used for any purpose other than in connection with a definitely related Government procurement operation, the United States Government thereby incurs no responsibility nor any obligation whatsoever; and the fact that the Government may have formulated, furnished, or in any way supplied the said drawings, specifications, or other data, is not to be regarded by implication or otherwise as in any manner licensing the holder or any other person or corporation, or conveying any rights or permission to manufacture, use, or sell any patented invention that may in any way be related thereto.

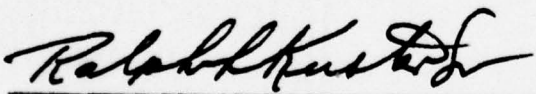
This report has been reviewed by the Information Office (OI) and is releasable to the National Technical Information Service (NTIS). At NTIS, it will be available to the general public, including foreign nations.

This technical report has been reviewed and is approved for publication.


DONALD P. RIZZETTA


CHARLES A. BAIR, JR., MAJOR, USAF
Chief, Analysis & Optimization Branch

FOR THE COMMANDER


RALPH L. KUSTER, JR., COLONEL, USAF
Chief, Structural Mechanics Division

Copies of this report should not be returned unless return is required by security considerations, contractual obligations, or notice on a specific document.

UNCLASSIFIED

SECURITY CLASSIFICATION OF THIS PAGE (When Data Entered)

19 REPORT DOCUMENTATION PAGE		READ INSTRUCTIONS BEFORE COMPLETING FORM	
1. REPORT NUMBER	2. GOVT ACCESSION NO.	3. RECIPIENT'S CATALOG NUMBER	
18 AFFDL-TR-77-126			
4. TITLE (and Subtitle)	5. TYPE OF REPORT & PERIOD COVERED		
6 THE AEROELASTIC ANALYSIS OF A TWO-DIMENSIONAL AIRFOIL IN TRANSONIC FLOW.	Technical Report		
	6. PERFORMING ORG. REPORT NUMBER		
7. AUTHOR(s)	8. CONTRACT OR GRANT NUMBER(s)		
10 Dr. Donald P. Rizzetta	15 F33615-76-C-3146		
9. PERFORMING ORGANIZATION NAME AND ADDRESS	10. PROGRAM ELEMENT, PROJECT, TASK AREA & WORK UNIT NUMBERS		
University of Dayton Research Institute Dayton, Ohio	16 PE 61102F WU 23070501 17 45		
11. CONTROLLING OFFICE NAME AND ADDRESS	12. REPORT DATE		
Air Force Flight Dynamics Laboratory (FBRB) AF Wright Aeronautical Laboratories, AFSC Wright-Patterson Air Force Base, Ohio 45433	11 December 1977		
14. MONITORING AGENCY NAME & ADDRESS (if different from Controlling Office)	13. NUMBER OF PAGES		
9 Final rept. Jul-Sep 77 12 56p.			
15. SECURITY CLASS. (of this report)		15a. DECLASSIFICATION/DOWNGRADING SCHEDULE	
UNCLASSIFIED			
16. DISTRIBUTION STATEMENT (of this Report)			
Approved for public release; distribution unlimited.			
17. DISTRIBUTION STATEMENT (of the abstract entered in Block 20, if different from Report)			
18. SUPPLEMENTARY NOTES			
19. KEY WORDS (Continue on reverse side if necessary and identify by block number)			
Transonic Flutter Unsteady Aerodynamics			
20. ABSTRACT (Continue on reverse side if necessary and identify by block number)			
A procedure is developed for the aeroelastic analysis of a two-dimensional airfoil in transonic flow. The fluid is assumed to be described by the unsteady low frequency small disturbance transonic potential equation for which a fully time implicit method of integration (LTRAN2) exists. Structural equations of motion for a three degree of freedom NACA 64A010 airfoil are integrated in time simultaneously with the unsteady potential equation using representative values of the structural parameters. The method is shown to be both stable and accurate, and the time response for several choices of initial conditions and reduced			

DD FORM 1 JAN 73 1473 EDITION OF 1 NOV 65 IS OBSOLETE

UNCLASSIFIED
SECURITY CLASSIFICATION OF THIS PAGE (When Data Entered)

105400 78 08 07 097LB

UNCLASSIFIED

SECURITY CLASSIFICATION OF THIS PAGE(When Data Entered)

Block 20: freestream density is presented. Oscillations with either increasing or decreasing amplitudes are found to result solely from the choice of initial conditions.

UNCLASSIFIED

SECURITY CLASSIFICATION OF THIS PAGE(When Data Entered)

FOREWORD

This report is the result of work carried out in the Optimization Group, Analysis and Optimization Branch, Structural Mechanics Division, Air Force Flight Dynamics Laboratory. It was performed by Dr. Donald P. Rizzetta, visiting scientist, under Project 2307, "Flight Vehicle Dynamics", Task 05, "Basic Research in Aeroelasticity". Dr. James J. Olsen is the AFFDL Task Engineer.

Dr. Rizzetta performed the work from July through September, 1977 and released the report in October 1977.

ACCESSION FOR	
NYS	<input checked="" type="checkbox"/>
DDI	<input type="checkbox"/>
ENGINEERING	<input type="checkbox"/>
ADMINISTRATION	<input type="checkbox"/>
BY	
DISTRIBUTION/AVAILABILITY CODES	
DIST.	AVAIL. CODE or SPECIAL
A	

TABLE OF CONTENTS

<u>SECTION</u>		<u>PAGE</u>
I	INTRODUCTION	1
II	GOVERNING EQUATIONS	3
	2.1 Structural Equations of Motion	3
	2.2 Unsteady Transonic Potential Equation	7
III	THE METHOD OF SOLUTION	11
IV	RESULTS	14
	4.1 Details of the Computations and Accuracy of the Solutions	14
	4.2 The One Degree of Freedom Case	19
	4.3 The Three Degree of Freedom Case	21
V	CONCLUSIONS AND RECOMMENDATIONS	42
	REFERENCES	44

PRECEDING PAGE BLANK

LIST OF ILLUSTRATIONS

<u>FIGURE</u>	<u>PAGE</u>
1. Airfoil with Plunge, Pitch, and Aileron Degrees of Freedom	4
2. Comparison of Forced and Free Oscillations for $M_\infty = 0.72$	16
3. Initial Surface Pressure Distribution for $M_\infty = 0.82$	17
4. Unsteady Pitching Displacement for Single Degree of Freedom Airfoil with $\alpha'(0) = 1$	20
5. Unsteady Pitching Moment for Single Degree of Freedom Airfoil with $\alpha'(0) = 1$	22
6. Unsteady Pitching Displacement for Single Degree of Freedom Airfoil with $\mu = 100$	23
7. Unsteady Pitching Moment for Single Degree of Freedom Airfoil with $\mu = 100$	24
8. Unsteady Plunging Displacement for Three Degree of Freedom Airfoil with $\alpha'(0) = 1$	25
9. Unsteady Pitching Displacement for Three Degree of Freedom Airfoil with $\alpha'(0) = 1$	26
10. Unsteady Aileron Displacement for Three Degree of Freedom Airfoil with $\alpha'(0) = 1$	27
11. Unsteady Lift for Three Degree of Freedom Airfoil with $\alpha'(0) = 1$	29
12. Unsteady Pitching Moment for Three Degree of Freedom Airfoil with $\alpha'(0) = 1$	30
13. Unsteady Aileron Moment for Three Degree of Freedom Airfoil with $\alpha'(0) = 1$	31
14. Unsteady Plunging Displacement for Three Degree of Freedom Airfoil with $\mu = 25$	32
15. Unsteady Pitching Displacement for Three Degree of Freedom Airfoil with $\mu = 25$	33
16. Unsteady Aileron Displacement for Three Degree of Freedom Airfoil with $\mu = 25$	34
17. Unsteady Lift for Three Degree of Freedom Airfoil with $\mu = 25$.	36

LIST OF ILLUSTRATION (CONTD)

<u>FIGURE</u>	<u>PAGE</u>
18. Unsteady Pitching Moment for Three Degree of Freedom Airfoil with $\mu = 25$	37
19. Unsteady Aileron Moment for Three Degree of Freedom Airfoil with $\mu = 25$	38
20. Surface Pressure Distribution for Three Degree of Freedom Airfoil with $\mu = 25$ at $N = 315$	39
21. Extended Time History of Unsteady Displacements for Three Degree of Freedom Airfoil with $\alpha'(0) = 5$ and $\mu = 25$	40
22. Extended Time History of Unsteady Aerodynamic Coefficients for Three Degree of Freedom Airfoil with $\alpha'(0) = 5$ and $\mu = 25$	41

LIST OF SYMBOLS

<u>SYMBOL</u>	<u>DEFINITION</u>
c	airfoil chord
C	unsteady aerodynamic force vector
C_l	section lift coefficient
C_m	section moment coefficient
C_p	section pressure coefficient, $(p-p_\infty)/1/2 \rho_\infty U_\infty^2$
D_o, D_α, D_β	uncoupled damping coefficients
D	structural damping matrix
f	non-dimensional airfoil geometric function
F	unsteady airfoil boundary
h	physical airfoil plunging displacement
H	unit step function
I_α, I_β	second mass moments
K_o, K_α, K_β	spring stiffness constants
K	structural stiffness matrix
m	linear airfoil mass distribution
M	total airfoil mass
M_∞	freestream Mach number
M	structural mass matrix
N	number of time steps
S_α, S_β	first mass moments
t	physical time
U_∞	freestream velocity
x	physical streamwise Cartesian coordinate
X	time dependent response sector
X_1	X

LIST OF SYMBOLS (CONTD)

<u>SYMBOL</u>	<u>DEFINITION</u>
x_2	x'
y	physical normal Cartesian coordinate
α	non-dimensional airfoil pitching displacement
β	non-dimensional aileron pitching displacement
γ	specific heat ratio
δ	maximum airfoil thickness to chord ratio
$\Delta\tau$	computational time step
$\Delta\xi$	computational streamwise mesh step size
$\Delta\eta$	computational normal mesh step size
$\zeta_\sigma, \zeta_\alpha, \zeta_\beta$	non-dimensional damping coefficients
η	non-dimensional normal Cartesian coordinate
μ	non-dimensional freestream density
ξ	non-dimensional streamwise Cartesian coordinate
$\bar{\xi}_o, \bar{\xi}_f$	non-dimensional first mass moments
ξ_o^*, ξ_f^*	non-dimensional second mass moments
ρ_∞	freestream density
σ	non-dimensional airfoil plunging displacement
τ	non-dimensional time
ϕ	non-dimensional perturbation velocity potential function
Φ	physical velocity potential function
ω	oscillation frequency
$\omega_\sigma, \omega_\alpha, \omega_\beta$	non-dimensional oscillation frequencies

SUBSCRIPTS

<u>SUBSCRIPT</u>	<u>DEFINITION</u>
a	evaluated at or referring to $x = x_a$
f	evaluated at or referring to $x = x_f$
h	evaluated at or referring to $x = x_h$
o	evaluated at or referring to $x = x_o$
min	minimum value
α	referring to airfoil pitch
δ	referring to aileron rotation
σ	referring to airfoil plunge
+	evaluated on airfoil upper surface
-	evaluated on airfoil lower surface

SECTION I

INTRODUCTION

For the case of flow over an airfoil in a freestream at Mach numbers near 1, small amplitude motions of the body surface can produce large variations in the aerodynamic forces and moments acting on the structure. In addition, phase differences between the flow variables and the resultant forces may be great. These characteristics tend to enhance the probability of encountering aeroelastic instabilities in the transonic flow regime and thus evidence a need for techniques of analyzing both the flow field and the structural response for such situations.

In the subsonic or supersonic case, the leading order flow equations are linear such that the aerodynamic forces depend upon the body motion in a linear fashion. Furthermore, the resultant forces acting on the airfoil may be obtained through superposition by summing the contributions due to the various types of body motion being considered. This allows the linear structural equations of motion to be solved independently of the aerodynamic equations which provide only the force coefficients. Uncoupling of the fluid and structural equations is not, in general, possible for the transonic regime due to its inherent nonlinear nature.

Advances in computational methods (1-16) have made a number of techniques available for computing unsteady transonic flows. While several different physical problems have been considered, the unsteady body motion was generally prescribed as a known function of time thereby precluding the simulation of aeroelastic behavior. It is only recently that the application of these computational procedures to actual aeroelastic problems has appeared (17,18).

It is the purpose of this report to describe a method for analyzing the structural response of a two-dimensional airfoil

in transonic flow, and to provide computational examples of the results obtained by applying this procedure to physical situations of practical interest. The governing aerodynamic equation of motion is assumed to be the unsteady low frequency small disturbance transonic equation for the velocity potential function which is capable of simulating nonlinear flow phenomena including irregular shock wave motions. Structural equations of motion are formulated for a three-degree of freedom airfoil by modelling the structure as a spring-mass system. The coupled aerodynamic-structural equations are then simultaneously integrated in time such that the flow field and the response of the airfoil to the resultant aerodynamic forces are allowed to interact in a manner much like the physical situation.

The method of time integration has already been applied in a superficial manner for analyzing a one degree of freedom airfoil (17). In this previous work, several types of motion were produced by varying the structural parameters. An alternative point of view is taken in this report. Here, the structural parameters are presumed fixed and the motion resulting from various choices of the initial conditions is considered. The airfoil selected for study is an NACA 64A010 airfoil which is 10% thick and representative of transonic airfoils currently in use. Plunging, airfoil pitching, and aileron rotation degrees of freedom have been allowed and structural parameters have been assigned representative values. Solutions were obtained for several choices of initial conditions and non-dimensional freestream density. The effects of these parameters on the time-dependent structural response and aerodynamic coefficients is presented.

SECTION II

GOVERNING EQUATIONS

In this section the structural equations of motion for a three degree of freedom airfoil used to simulate aeroelastic behavior are developed. These are formulated in a manner compatible with the aerodynamic equation such that the coupled system may be integrated in time. The governing aerodynamic equation for unsteady transonic flow is summarized along with its inherent assumptions.

2.1 Structural Equations of Motion

An airfoil which is allowed to have three degrees of freedom, namely, plunge, pitch, and aileron rotation were selected as being representative of aeroelastic problems commonly occurring in transonic flows. Elastic properties of such an airfoil were modelled by the spring-mass system depicted in Figure 1. The airfoil of chord c and maximum thickness to chord ratio δ with nose at the origin and aileron leading edge located at x_f is restrained by a linear spring such that it is free to oscillate in plunge about $y = 0$ with a displacement h . Torsional springs are attached at $x = x_o$ and $x = x_h$. The pitching of the airfoil and control surface rotation are given by α and β respectively where it is noted that β is referenced from the rotated airfoil surface. Only uncoupled damping is allowed.

If K_o, K_α , and K_β are the respective spring stiffness, D_o, D_α , and D_β the assumed uncoupled damping coefficients, and $m(x)$ the linear mass distribution, then it can be shown (19) that the physical equations for the system are the following:

$$M \frac{d^2 h}{dt^2} + S_\alpha \frac{d^2 \alpha}{dt^2} + S_\beta \frac{d^2 \beta}{dt^2} + D_o \frac{dh}{dt} + K_o h = \rho_\infty U_\infty^2 c^2 C_\ell(t)/2, \quad (1)$$

$$S_{\alpha} \frac{d^2 h}{dt^2} + I_{\alpha} \frac{d^2 \alpha}{dt^2} + [(x_0 - x_f) S_{\beta} + I_{\beta}] \frac{d^2 \beta}{dt^2} + D_{\alpha} \frac{d\alpha}{dt} \quad (2)$$

$$+ K_{\alpha} \alpha = \rho_{\infty} U_{\infty}^2 c^3 C_{m0}(t)/2,$$

$$S_{\beta} \frac{d^2 h}{dt^2} + [(x_0 - x_f) S_{\beta} + I_{\beta}] \frac{d^2 \alpha}{dt^2} + I_{\beta} \frac{d^2 \beta}{dt^2} + D_{\beta} \frac{d\beta}{dt} \quad (3)$$

$$+ K_{\beta} \beta = \rho_{\infty} U_{\infty}^2 c^3 C_{mh}(t)/2,$$

where

$$M = \int_0^c m(x) dx, \quad (4)$$

$$S_{\alpha} = \int_0^c (x_0 - x) m(x) dx, \quad (5)$$

$$S_{\beta} = \int_{x_f}^c (x_h - x) m(x) dx, \quad (6)$$

$$I_{\alpha} = \int_0^c (x_0 - x)^2 m(x) dx, \quad (7)$$

and

$$I_{\beta} = \int_{x_f}^c (x_h - x)^2 m(x) dx. \quad (8)$$

These can be put into a convenient non-dimensional form by defining:

$$\xi = x/c, \quad (9)$$

$$\tau = U_{\infty} \delta^{2/3} t / c, \quad (10)$$

$$\sigma = h/c, \quad (11)$$

$$\bar{\xi}_0 = S_\alpha / cM, \quad (12)$$

$$\bar{\xi}_f = S_\beta / cM, \quad (13)$$

$$\xi_O^* = I_\alpha / c^2 M, \quad (14)$$

$$\xi_f^* = I_\beta / c^2 M, \quad (15)$$

$$\omega_h = (c^2 K_O / J_\omega^2 M)^{1/2}, \quad (16)$$

$$\omega_\alpha = (K_\alpha / U_\omega^2 \xi_O^* M)^{1/2}, \quad (17)$$

$$\omega_\beta = (K_\beta / U_\omega^2 \xi_f^* M)^{1/2}, \quad (18)$$

$$\zeta_O = D_O / 2\omega_h M, \quad (19)$$

$$\zeta_\alpha = D_\alpha / 2\omega_\alpha I_\alpha, \quad (20)$$

$$\zeta_\beta = D_\beta / 2\omega_\beta I_\beta, \quad (21)$$

and

$$\mu = 2M / \rho_\omega c^3. \quad (22)$$

If these are substituted into equations (1) - (3), then the following result:

$$\begin{aligned} \sigma''(\tau) + \bar{\xi}_O \alpha''(\tau) + \bar{\xi}_f \beta''(\tau) + 2\delta^{-2/3} \omega_O \zeta_O \sigma'(\tau) \\ + \delta^{-4/3} \omega_O^2 \sigma(\tau) = \delta^{-4/3} C_\ell(\tau) / \mu, \end{aligned} \quad (23)$$

$$\begin{aligned} \bar{\xi}_0 \sigma''(\tau) + \xi_0^* \alpha''(\tau) + [(\xi_0 - \xi_f) \bar{\xi}_f + \xi_f^*] \beta''(\tau) + 2\delta^{-2/3} \omega_\alpha \zeta_\alpha \alpha'(\tau) \\ + \delta^{-4/3} \xi_0^* \omega_\alpha^2 \alpha(\tau) = \delta^{-4/3} C_{mo}(\tau) / \mu, \end{aligned} \quad (24)$$

$$\begin{aligned} \bar{\xi}_f \sigma''(\tau) + [(\xi_0 - \xi_f) \bar{\xi}_f + \xi_f^*] \alpha''(\tau) + \xi_f^* \beta''(\tau) + 2\delta^{-2/3} \omega_\beta \zeta_\beta \beta'(\tau) \\ + \delta^{-4/3} \xi_f^* \omega_\beta^2 \beta(\tau) = \delta^{-4/3} C_{mh}(\tau) \mu. \end{aligned} \quad (25)$$

The system (23) - (25) may be written as the vector equation

$$MX''(\tau) + DX'(\tau) + KX(\tau) = C(\tau) / \mu \quad (26)$$

where the initial conditions $X(0)$ and $X'(0)$ complete a description of the problem.

2.2 Unsteady Transonic Potential Equation

A number of procedures are available for the solution of unsteady transonic flow problems. Methods of harmonic analysis (3-7) assume that the unsteady flow may be considered as a small perturbation about a steady state due to the motion of the boundary. These time-linearized methods fail to treat shock motions exactly and thus are limited in application to very small amplitude airfoil motions which constrain shock waves to small displacement about their steady-state position. In addition, the unsteady perturbations are prescribed to have a harmonic dependence in time. While such methods are not capable of treating general airfoil motions, they can provide input for classical aeroelastic computations (18).

A more exact treatment of unsteady transonic flow problems is provided by integrating the equations of motion in time. Solutions to the unsteady Euler equations (8,9) and the full potential equation (10) have been obtained by explicit finite difference schemes. Although these methods can in principle be applied to quite general airfoil motions, they are limited by a time step restriction for computational stability thereby making practical calculations prohibitive. If consideration is limited to irrotational flows and low frequency motions, then a reduced form of the unsteady potential equation results. A fully time-implicit

method of solution of this equation has been developed (17) such that no time step restriction for stability exists. In addition, this equation is capable of simulating nonlinear flow phenomena including irregular shock wave motions. Solutions of the unsteady low frequency potential equation have compared quite well with solutions of the Euler equations (17).

We now consider the two-dimensional irrotational unsteady flow over an airfoil. The velocity potential function, ϕ , is expanded as

$$\phi(x, y, t) = u_{\infty} c \delta^{2/3} \phi(\xi, \eta, \tau) \quad (27)$$

where

$$\eta = y \delta^{1/3} / c, \quad (28)$$

ξ and τ are given by equations (9) and (10) respectively, and it is assumed that $\delta \ll 1$. If these expressions are substituted into the full unsteady potential equation and the coefficients of like powers of δ are equated, then the leading order result is

$$[(1 - M_{\infty}^2) \delta^{-2/3} - (1 + \gamma) M_{\infty}^2 \phi_{\xi}] \phi_{\xi\xi} + \phi_{\eta\eta} = 2 M_{\infty}^2 \phi_{\xi\tau} \quad (29)$$

if it is assumed that $(1 - M_{\infty}^2) \delta^{-2/3} = O(1)$.

This is the form of the unsteady low frequency small disturbance transonic potential equation which will be considered appropriate for describing the flow. Corresponding boundary conditions for equation (29) are obtained from the flow tangency condition on the airfoil surface, from the Kutta condition at the trailing edge with a constant jump in potential across the vortex sheet in the wake, and by requiring the perturbation velocity to vanish far from the body.

The unsteady airfoil boundary is defined by

$$y - F(x, t) = 0 \text{ for } 0 \leq x \leq c. \quad (30)$$

Here

$$F(x,t) = c\delta[f(\xi) + \alpha(t)/\delta - (\xi - \xi_0)\alpha(t)/\delta - (\xi - \xi_h)H(\xi - \xi_f)\beta(t)/\delta] \quad (31)$$

where $f(\xi)$ corresponds to the specified airfoil geometry; α , α , and β are the previously defined plunging, airfoil pitching, and aileron pitching displacements respectively; and $H(\xi - \xi_f)$ is the unit step function. With this, the flow tangency condition becomes

$$\phi_\eta = f'(\xi) - \alpha(t)/\delta - H(\xi - \xi_f)\beta(t)/\delta \text{ on } \eta = 0 \text{ for } 0 \leq \xi \leq 1. \quad (32)$$

We note that this condition is applied on $\eta = 0$ as is consistent with the small disturbance assumption. In addition, to the order considered in equation (29) there is no explicit dependence on σ in the surface boundary condition (32). The wake condition is applied as

$$[\phi_\xi] = 0 \text{ on } \eta = 0 \text{ for } \xi > 1 \quad (33)$$

where the square brackets indicate the "jump" in the enclosed quantity and the condition is again applied along $\eta = 0$. The farfield boundary condition is

$$(\phi_\xi)^2 + (\phi_\eta)^2 \rightarrow 0 \text{ as } \xi^2 + \eta^2 \rightarrow \infty. \quad (34)$$

so that equation (29) and corresponding boundary conditions (32)-(34) complete a description of the flow field problem if an initial profile, $\phi(\xi, \eta, 0)$, is specified.

With this formulation, the unsteady pressure coefficient is given by

$$C_p = -2\delta^{2/3}\phi_\xi. \quad (35)$$

The corresponding lift and moment coefficients follow as

$$C_\ell = \int_0^1 (C_{p-} - C_{p+}) d\xi, \quad (36)$$

$$c_{mo} = \int_0^1 (c_{p-} - c_{p+}) (\xi_o - \xi) d\xi, \quad (37)$$

and

$$c_{mh} = \int_{\xi_f}^1 (c_{p-} - c_{p+}) (\xi_h - \xi) d\xi. \quad (38)$$

SECTION III

THE METHOD OF SOLUTION

We now seek a method of obtaining solutions to the coupled system, equation (26) with appropriate initial conditions and equation (29) with boundary conditions (32)-(34) and initial profile $\phi(\xi, \eta, 0)$. This formulation will be considered general with respect to equation (26) such that any number of degrees of freedom are permitted. Equation (26) is first written as an equivalent first order system by defining

$$X_1(\tau) = X(\tau) \quad (39)$$

and

$$X_2(\tau) = X'(\tau) \quad (40)$$

so that

$$X_1'(\tau) = X_2(\tau) \quad (41)$$

and

$$X_2'(\tau) = M^{-1} [C(\tau)/\mu - \mathcal{D}X_2(\tau) - KX_1(\tau)]. \quad (42)$$

Equations (41) and (42) were then solved by a 4-point Adams-Moulton integration in time (20). This is an implicit predictor-corrector technique having a local truncation error of order $(\Delta\tau)^4$. A number of other methods, both explicit and implicit, were tried. It was found that when coupled with the aerodynamic equation, calculations eventually became unstable for central difference and 3-term Taylor series explicit schemes and for Euler-Cauchy and Milne 3-point implicit schemes, even when extremely small time steps were employed. A Milne 5-point implicit technique with local

truncation error of order $(\Delta \tau)^6$, although stable, appeared to produce less accuracy than the Adams-Moulton integration.

It will be of interest to compare some time integrated results with homogeneous solutions to the structural system. In particular, for $\mu \rightarrow \infty$, the homogeneous result should be recovered. For the case of $C(\tau) = 0$ the associated eigenvalue problem corresponding to equations (41) and (42) was considered and the eigenvalues and eigenvectors obtained. The solution vector was then represented as the linear combination of the eigenvectors which satisfied the specified initial conditions. These solutions are thus considered "exact" as they are free of truncation error which is present in time integrated results. No attempt was made to obtain normal modes as this is not in general possible for arbitrary values of the mass, damping, and stiffness matrices (M, D, K) (21).

An efficient time-implicit finite difference algorithm (13) has been developed for obtaining solutions to the low frequency transonic equation. This technique was incorporated in the computer code LTRAN2, developed by Ballhaus and Goorjian (16) for the purpose of computing unsteady transonic flows over airfoils using the form of the potential equation given by (29). Several minor changes in the basic code were necessary in order to accommodate a simultaneous solution of the structural equations (41) and (42). Details of LTRAN2 are briefly summarized here.

The basic LTRAN2 code employs a non-iterative alternating-direction implicit (ADI) scheme to advance the solution for the perturbation potential, ϕ , from one time level to the next at each grid point in the computational flow field. Differencing in the ξ -direction is of the mixed type which has been quite successful in maintaining stability for both subsonic and supersonic flow regions. Conservation form of the equation is preserved, which is essential for a proper description of shock wave motions. While the ADI scheme has no time step limitation for stability based upon classical linear stability analysis, instabilities may be generated by the motion of shock waves due to the mixed differencing. Thus, $\Delta \tau$ must be chosen such that shock

waves do not travel more than one mesh point in the ξ - direction over a single time step. A cubic spline is used to approximate the airfoil geometric function $f(\xi)$, which is usually provided as tabular data for NACA airfoils. Aerodynamic moments are evaluated by Simpson's rule integration according to equations (36) - (38). A smooth non-uniform computational mesh which is symmetric about $\eta = 0$ is employed. The grid spacing is such that points are clustered near the airfoil leading and trailing edges in the ξ - direction, and near $\eta = 0$ in the η - direction. Mesh boundaries are taken sufficiently far from the airfoil such that condition (34) may be approximated. The airfoil surface is described by 33 mesh points. Details of the grid system are the following:

- a. number of ξ -points = 99
- b. number of η -points = 79
- c. $\Delta\xi_{\min} = 0.00330$
- d. $\Delta\eta_{\min} = 0.02000$
- e. $-1033.53047 \leq \xi \leq 855.91313$
- f. $-811.12200 \leq \eta \leq 811.12200$.

Results of computations from LTRAN2 have been shown to compare well with solutions of the time-dependent Euler equations, and have reproduced unsteady transonic behavior which has commonly been observed experimentally (16). In order to accommodate the simultaneous solution of the structural equations (41) and (42) it was necessary to modify LTRAN2 such that the time marching technique is now a two-step (predictor-corrector) procedure. Although this in effect doubles the computing time for a fixed Δt , without this modification stable calculations could not in general be obtained.

SECTION IV

RESULTS

In this section the behavior of numerical solutions obtained by the method outlined in Section 3.0 is considered. Accuracy of the solutions is discussed and the choice of structural parameters indicated. Results are presented for an airfoil having both one and three degrees of freedom. Solutions were obtained for fixed initial conditions and several values of the reduced density, μ . Additional results indicate that for μ fixed, stable or unstable motion can be produced solely by the choice of initial conditions. All of the calculations presented here correspond to an NACA 64A010 airfoil.

4.1 Details of the Computations and Accuracy of the Solutions

In order to indicate the stability of the computational method, it will be demonstrated that an exact solution of the coupled aeroelastic system of equations can be reliably reproduced by time integration. For this purpose, the airfoil motion was forced for three periods of oscillation according to the prescribed functions.

$$\sigma(\tau) = \alpha(\tau) = \beta(\tau) = 0.01745 \sin(4.3\tau). \quad (43)$$

Using a steady-state profile as the initial condition, equation (29) was integrated in time by LTRAN2. After a short period of time the effect of the initial conditions became negligible such that the aerodynamic forces, C_ℓ , C_{m_o} , and C_{m_h} were periodic. Analytical expressions for these forces were then extracted from numerical results and introduced into equations (41) and (42). The structural parameters comprising the mass, damping, and stiffness matrices (M, D, K) and the reduced density μ were then chosen such that the analytic solution to equations (41) and (42) was given by the previously prescribed functions (43) for forced motion. At this point the coupled system was integrated in time

using as initial values the conditions present when the forced motion was terminated.

This procedure was used to study both stability and accuracy characteristics of various numerical techniques for integrating the structural equations of motion. It was found that C_ℓ was the aerodynamic coefficient most sensitive to procedural variations. One result of this study is shown in Figure 2 for the case $M_\infty = 0.72$. The time dependent lift is displayed for both forced and free motion. Over three periods of free oscillation the variation in C_ℓ was never more than 0.5% and it appeared that the integration could have proceeded indefinitely without instability and with reasonable accuracy.

We now devote our attention to solutions of the coupled aeroelastic equations for representative choices of the structural parameters. Impulsive motion from an equilibrium state will be the only type of motion considered here. For all the results presented in this section, initial values correspond to

$$\sigma(0) = \alpha(0) = \beta(0) = 0,$$

$$\sigma'(0) = \beta'(0) = 0,$$

$$\alpha'(0) \text{ prescribed}$$

with $\phi(\xi, \eta, 0)$ given by the steady-state profile for $M_\infty = 0.82$. The initial pressure distribution for these results is shown in Figure 3. It is noted that this case is supercritical with a shock appearing between $\xi = 0.50$ and $\xi = 0.60$. It should be pointed out that solutions are not limited to the above initial values, however it was necessary to fix a certain number of parameters in order to conduct a reasonable study. Due to inherent nonlinearity in the transonic equation, various types of motion may result depending on the choice of $\alpha'(0)$. This is quite unlike classical flutter analysis. Physically, the initial conditions $\sigma'(0)$, $\alpha'(0)$, and $\beta'(0)$ may be interpreted as impulsive gusts striking the airfoil. By varying these initial conditions, stability boundaries may be established. Combinations of these

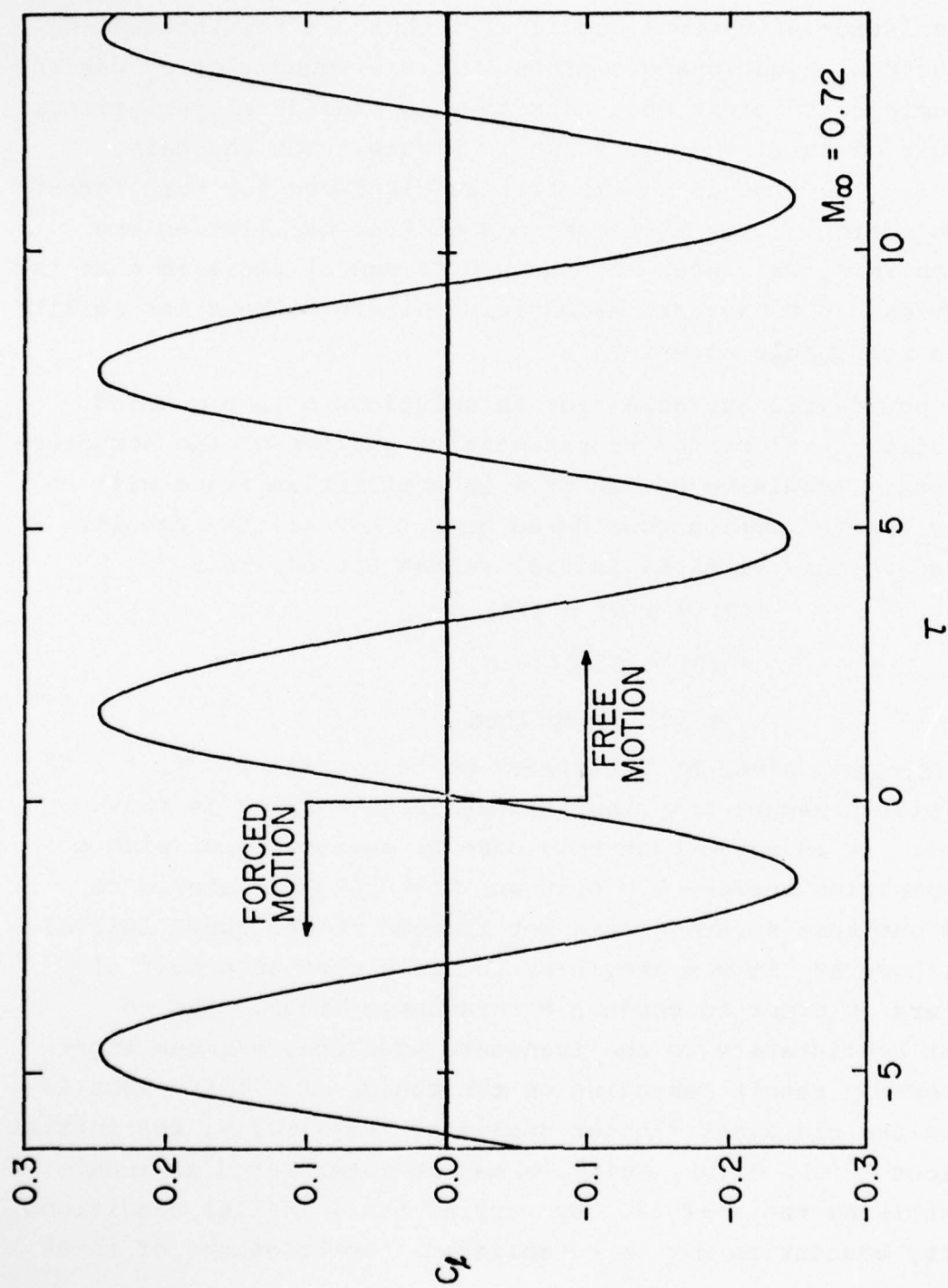


FIGURE 2. Comparison of Forced and Free Oscillations for $M = 0.72$

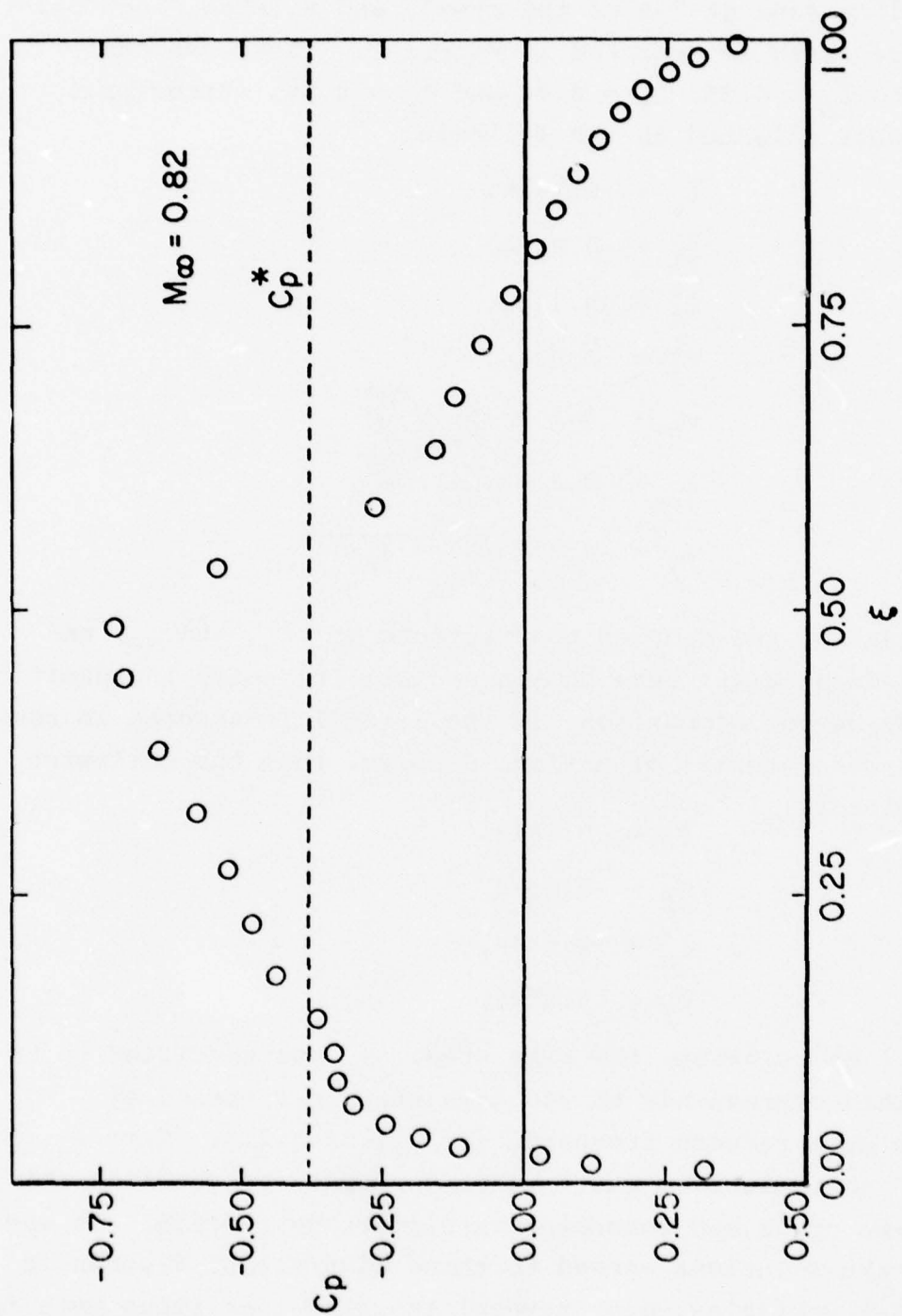


FIGURE 3. Initial Pressure Distribution for $M_\infty = 0.82$

conditions need necessarily be considered, however, as superposition cannot be applied.

The airfoil with pitch point located at the quarter chord aileron leading edge at 75% of the chord, and aileron hinge point at 80% of the chord is depicted in Figure 1. These choices correspond to $\xi_o = 0.25$, $\xi_f = 0.75$ and $\xi_h = 0.80$. Structural parameters were selected as the following:

$$\begin{aligned}\bar{\xi}_o &= -0.1818, \\ \bar{\xi}_f &= -0.0034, \\ \xi_o^* &= 0.1141, \\ \xi_f^* &= 0.0346, \\ \omega_o &= 0.1 = \left(\frac{c}{U_\infty}\right) \sqrt{\frac{K\alpha}{M}} \\ \omega_\alpha &= 0.2 = \left(\frac{c}{U_\infty}\right) \sqrt{\frac{K\alpha}{I_\alpha}} \\ \omega_\beta &= 0.3 = \left(\frac{c}{U_\infty}\right) \sqrt{K_\beta/I_\beta}.\end{aligned}$$

Various values of the damping coefficients (ζ_o , ζ_α , and ζ_β) and the reduced density (μ) were chosen and will be noted in specific results. By way of comparison, if the airfoil is assumed to consist of a homogenous material of uniform density, then the following may be obtained:

$$\begin{aligned}\bar{\xi}_o &= -0.1818, \\ \bar{\xi}_f &= -0.0034, \\ \xi_o^* &= 0.0846, \\ \xi_f^* &= 0.0052.\end{aligned}$$

and

For all calculations the time step, Δt , was specified to be 0.01745. This corresponds to 360 time steps per period of oscillation at a reduced frequency ($\omega c/U_\infty$) of 0.215. Time accuracy of the solutions was further confirmed by doubling this nominal value of Δt and comparing with previous results. It was found that the solutions agreed to three significant figures in all dependent variables, over several thousand time steps even for cases which exhibited unstable motion. When the time increment

was increased by a factor of five, however, the computations eventually became unstable. This was most likely due to a violation of the time step size limitation with respect to the motion of the shock across the computational mesh which was previously described. All calculations were performed on a CDC Cyber 74 computer and required approximately 20 minutes of computing time for every 1000 time steps.

4.2 The One Degree of Freedom Case

It is useful to study the behavior of solutions for a single degree of freedom airfoil. Because there are no superimposed modes of motion in this case, the characteristic details of the solution are quite clear. For an airfoil oscillating in pitch only, the structural system reduces to equation (24) with $\sigma = \beta = 0$. Figure 4 indicates the time response of the single degree of freedom airfoil for $\zeta_\alpha = 0.01$ and $\alpha'(0) = 1.0$ for two values of the reduced density. The homogeneous solution is also shown for comparison. Here the pitching displacement has been normalized by the impulsive pitch velocity such that the homogeneous solution is universal for all choices of $\alpha'(0)$. This will prove a convenient form to use for later results when variations in the initial condition are considered. The time axis is represented in terms of the number of time steps, N , in order to emphasize the fact that the resolution of the discretization in time is sufficient to consider the time history a continuum. The corresponding physical time is easily obtained from equation (10) as

$$t = c\Delta\tau\delta^{-2/3} N/u_\infty. \quad (44)$$

For the choices of $\Delta\tau$ and δ considered here this results in one chord length of airfoil travel for every 12.344 time steps.

With $\zeta_\alpha = 0.01$ it is seen that the homogeneous solution is very slightly damped. For $\mu = 50$, the time integrated solution varies slightly from the homogeneous result. In fact for $\mu = 100$ the homogeneous solution was recovered virtually intact. Once again this confirms accuracy of the numerical method. As the

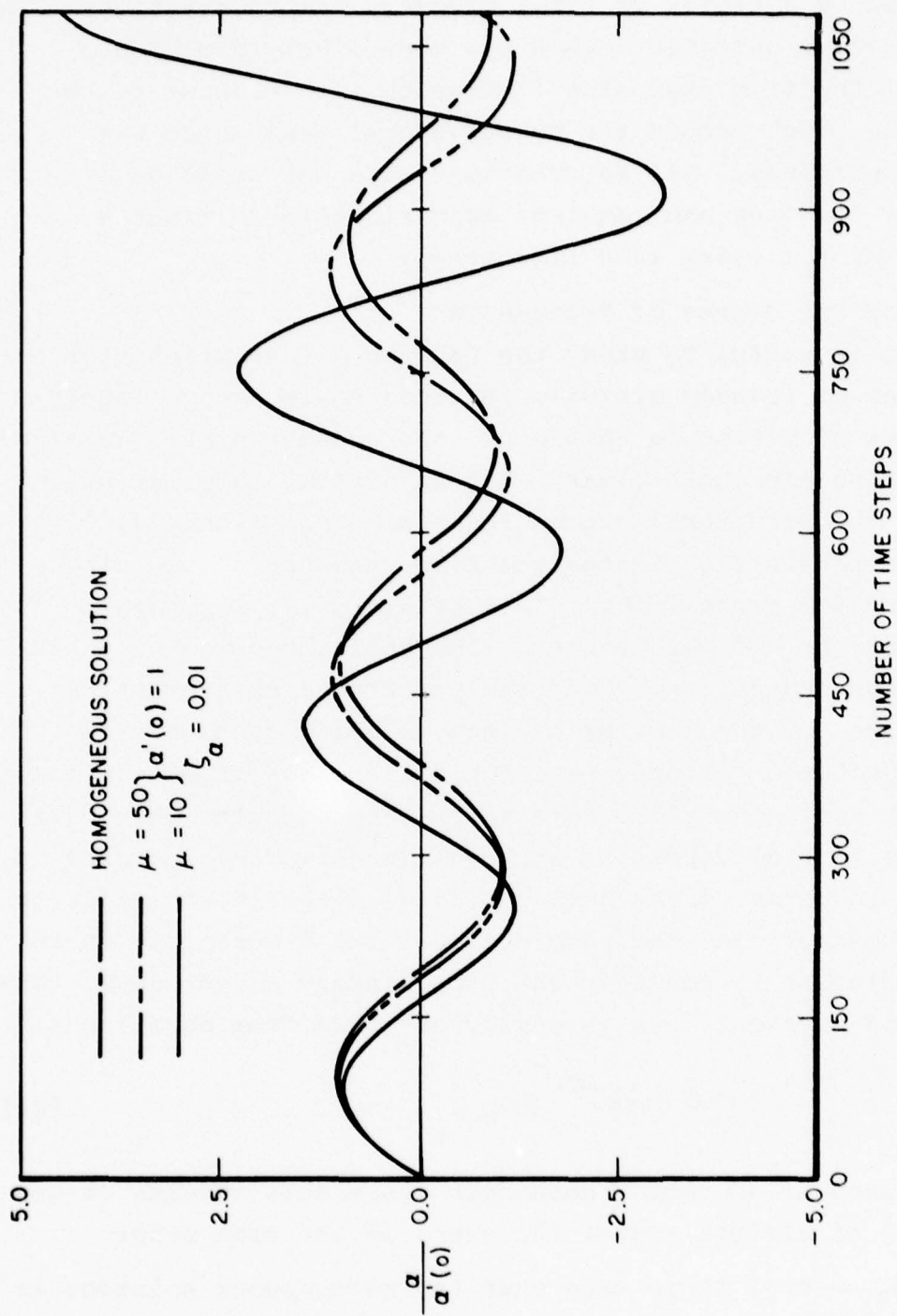


Figure 4. Unsteady Pitching Displacement for Single Degree of Freedom Airfoil with $\alpha'(0) = 1$.

reduced is increased, a shift in the oscillation frequency as well as well as an increase in amplitude is noted. Corresponding time histories for the moment coefficient about the pitch point are displayed in Figure 5, and are seen to exhibit a behavior similar to that of the pitching displacement.

For $\mu = 100$ and $\zeta_\alpha = 0.03$ the pitching displacement for several values of the initial condition is shown in Figure 6. The case $\alpha'(0) = 4.0$ is practically neutrally stable. It is seen that for $\alpha'(0) = 1.0$ the amplitude of oscillation is about 20% damped in two periods of oscillation. Slightly growing amplitudes are produced with $\alpha'(0) = 7.5$. This behavior exemplifies the nonlinear character of the coupled aeroelastic system. It is noted that no appreciable change in frequency is evident for variation in the initial conditions. Moment coefficients corresponding to these cases appear in Figure 7. For small time ($N < 200$), the anomalous behavior apparent in the cases $\alpha'(0) = 4.0$ and $\alpha'(0) = 7.5$ is most likely due to starting phenomena and an adjustment in the phase difference between α and C_{mo} .

4.3 The Three Degree of Freedom Case

We now focus our attention on the three degree of freedom airfoil. For the results considered in this section all damping coefficients were assigned the identical value of 0.03 (i.e., $\zeta_\sigma = \zeta_\alpha = \zeta_\beta = 0.03$). Unsteady displacements for the initial condition $\alpha'(0) = 1$ and several values of reduced density are given in Figures 8-10 with the homogeneous solution indicated for comparison. The plunging displacement shown in Figure 8 is seen to vary from the homogeneous result and experience a shift in frequency as μ increases. Damped motion appears to occur for $\mu = 100$ and $\mu = 50$, but an increasing amplitude is noted for $\mu = 25$. In Figure 9 this same behavior is observed for the pitching displacement. There seems to be very little shift in frequency for the cases $\mu = 100$ and $\mu = 50$. It appears that for large time the response is tending to make the plunge and pitch frequencies identical. Figure 10 indicates the aileron displacement for these cases. It is seen that there is apparently damped motion with very little frequency shift for all values of μ .

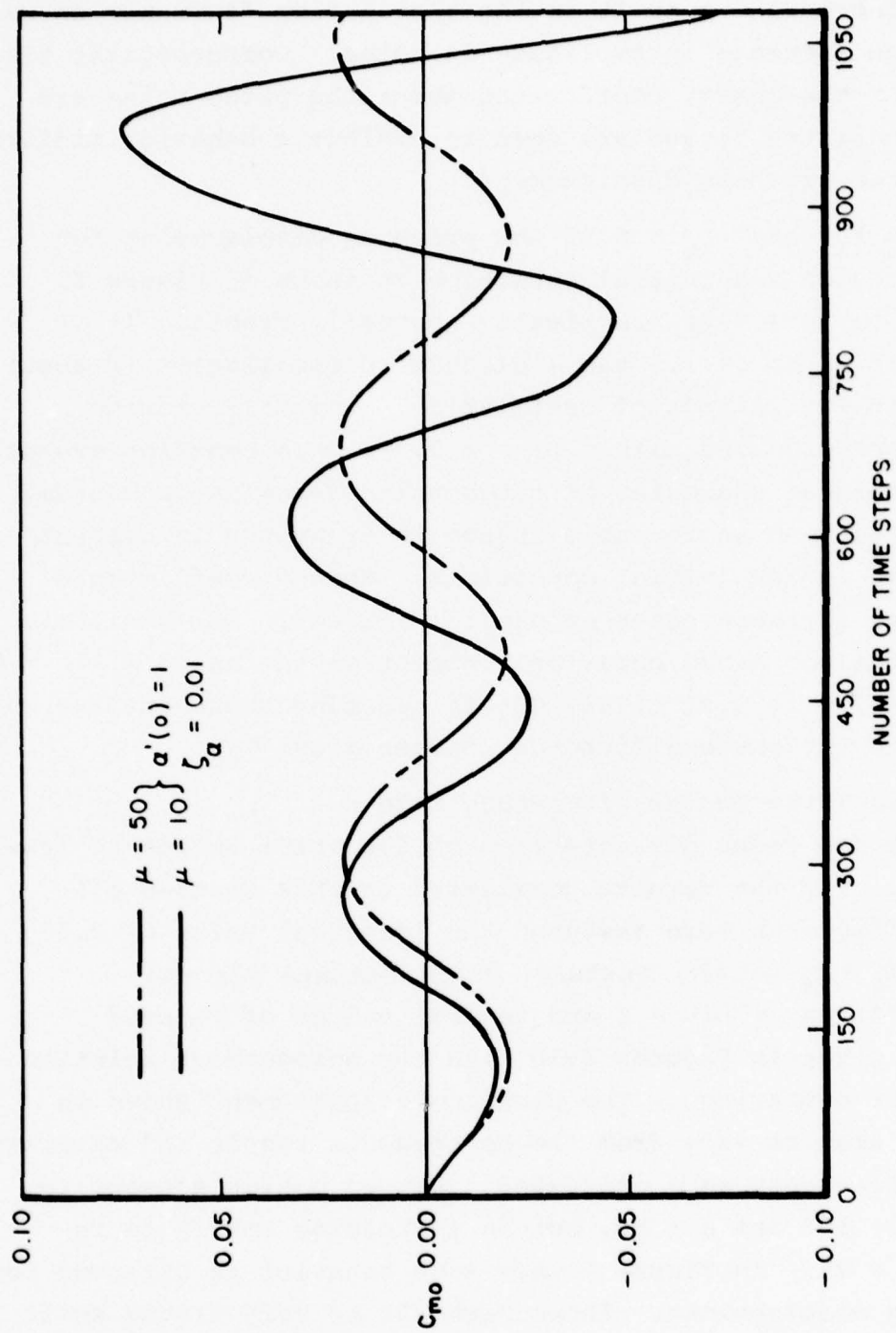


Figure 5. Unsteady Pitching Moment for Single Degree of Freedom Airfoil with $\alpha'(0) = 1$.

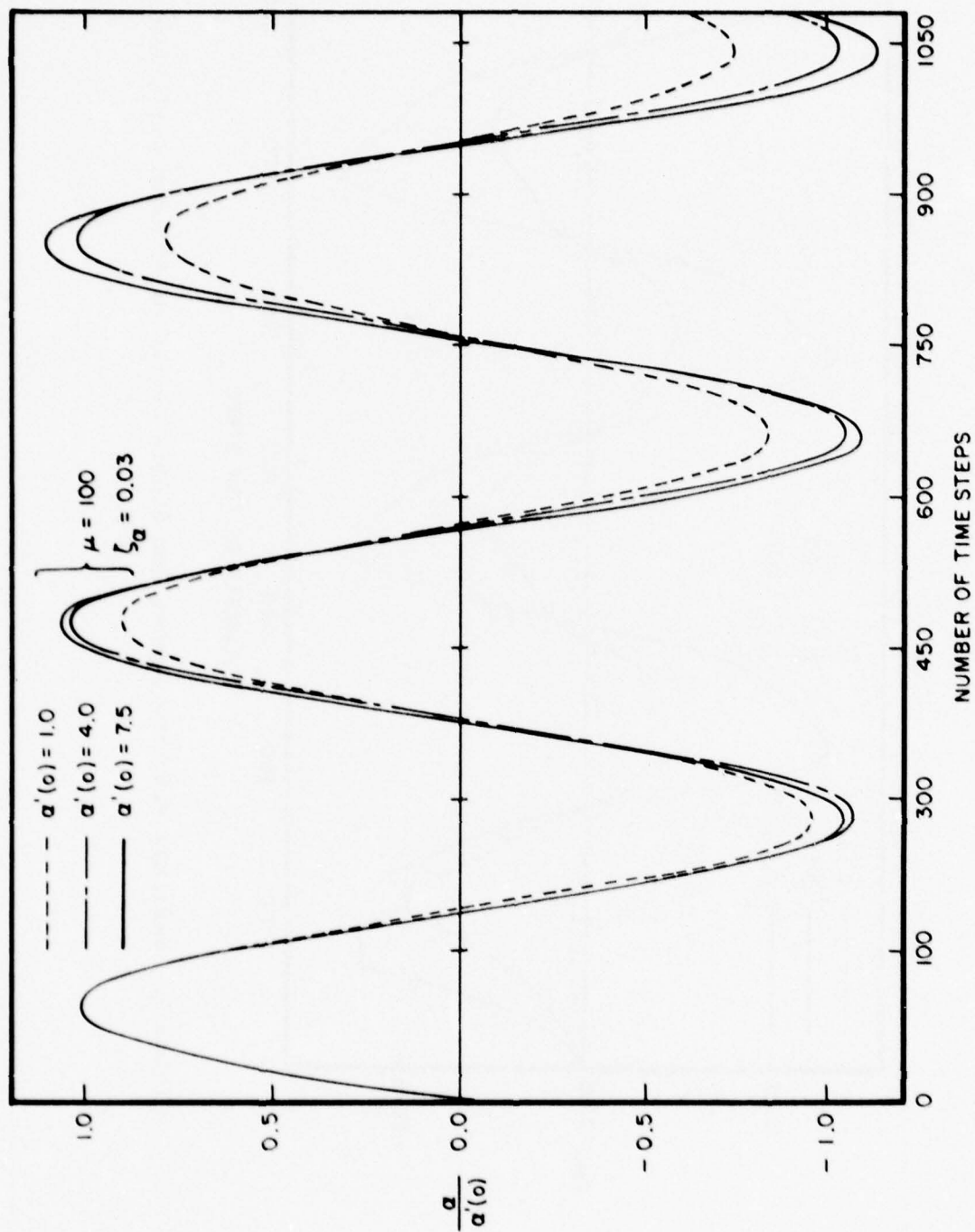


Figure 6. Unsteady Pitching Displacement for Single Degree of Freedom Airfoil with $\mu=100$.

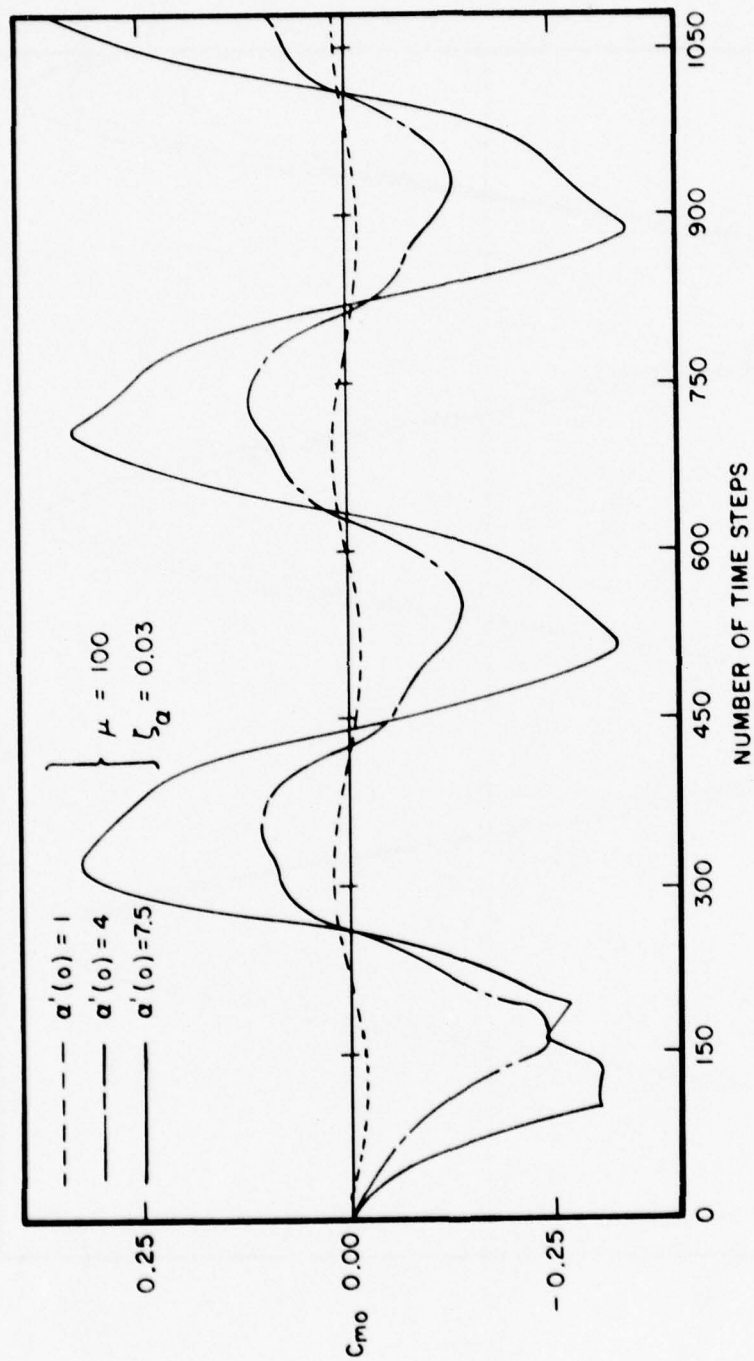


Figure 7. Unsteady Pitching Moment for Single Degree of Freedom Airfoil with $\mu=100$.

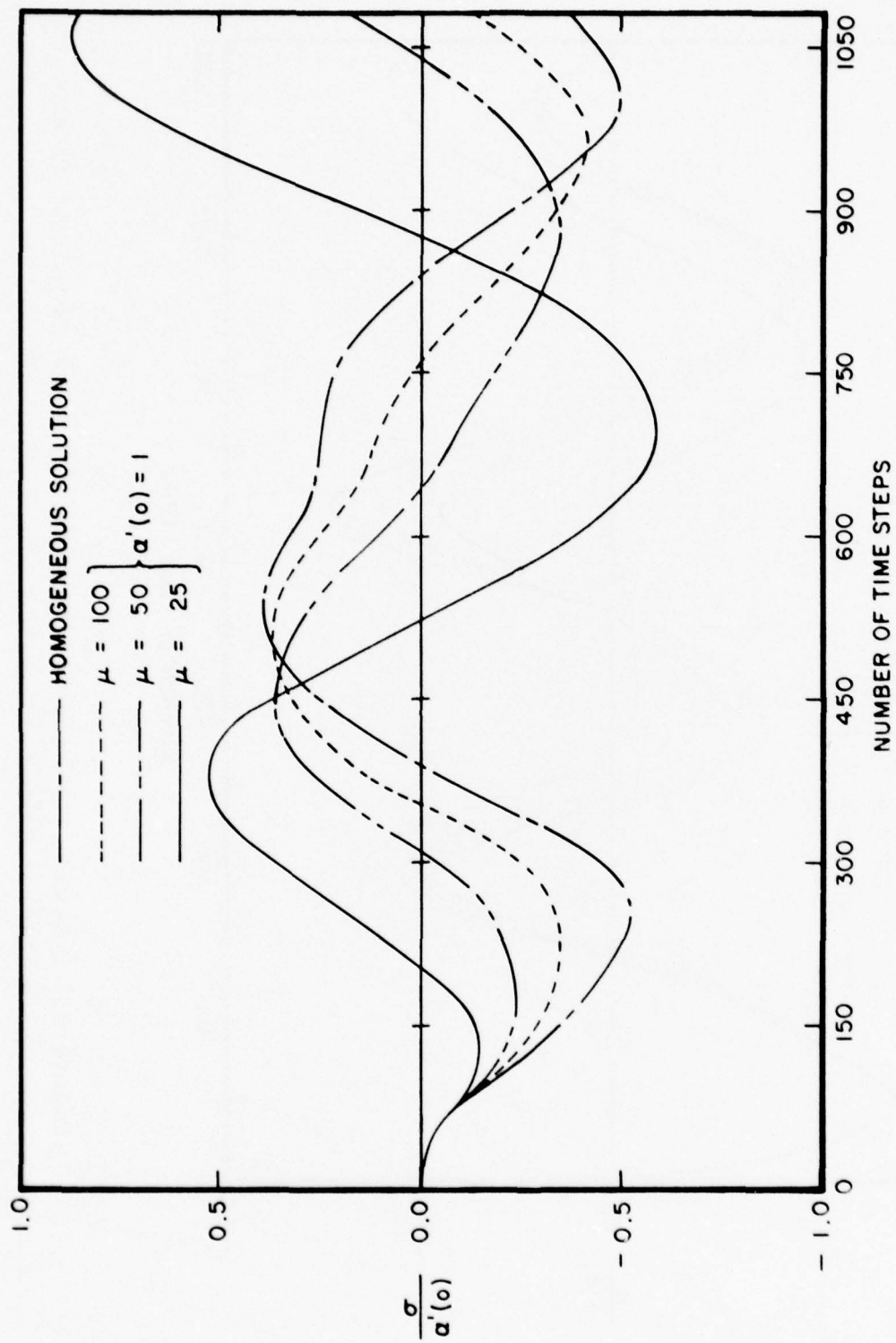


Figure 8. Unsteady Plunging Displacement for Three Degree of Freedom Airfoil with $\alpha'(0) = 1$.

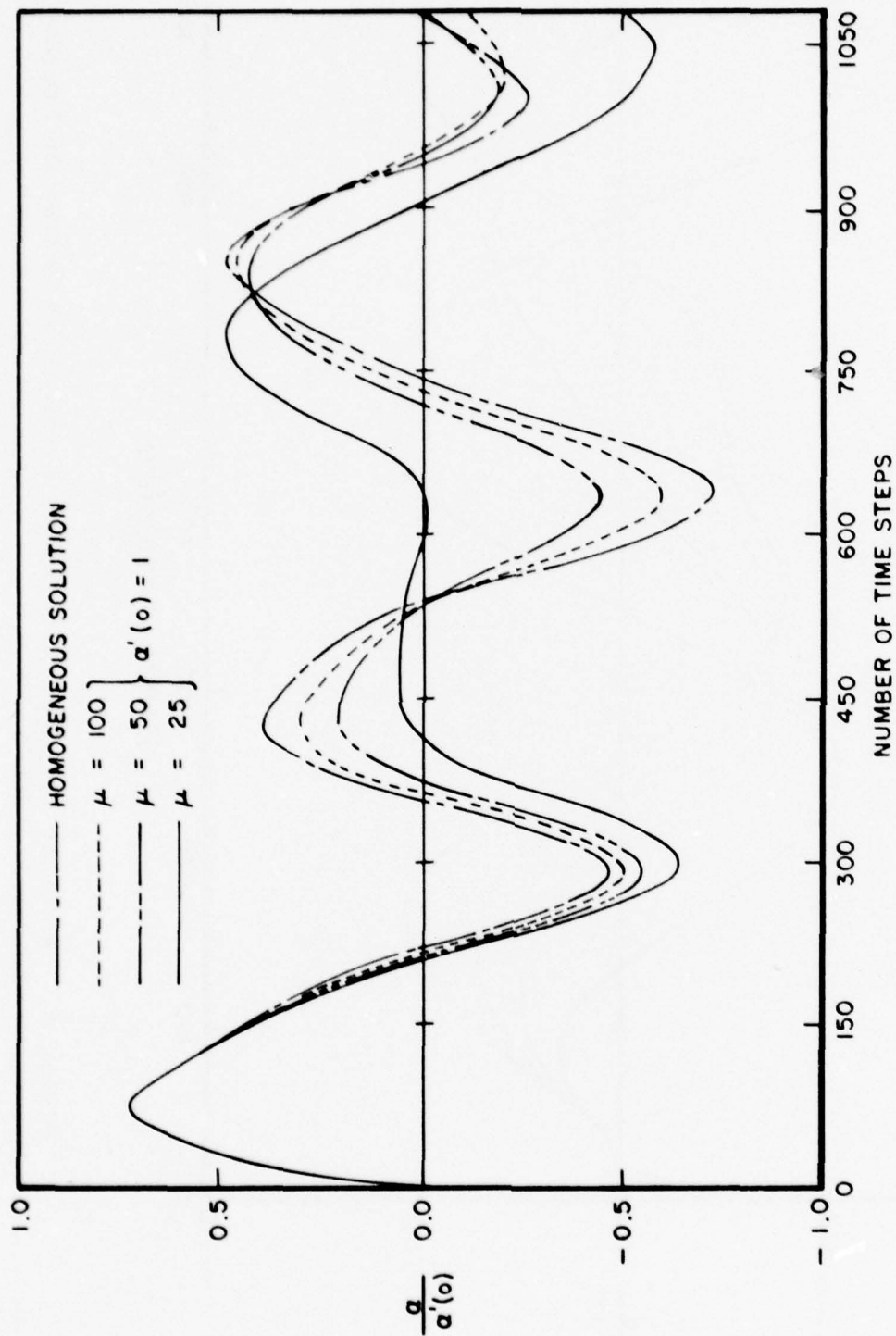


Figure 9. Unsteady Pitching Displacement for Three Degree of Freedom Airfoil with $\alpha'(0) = 1$.

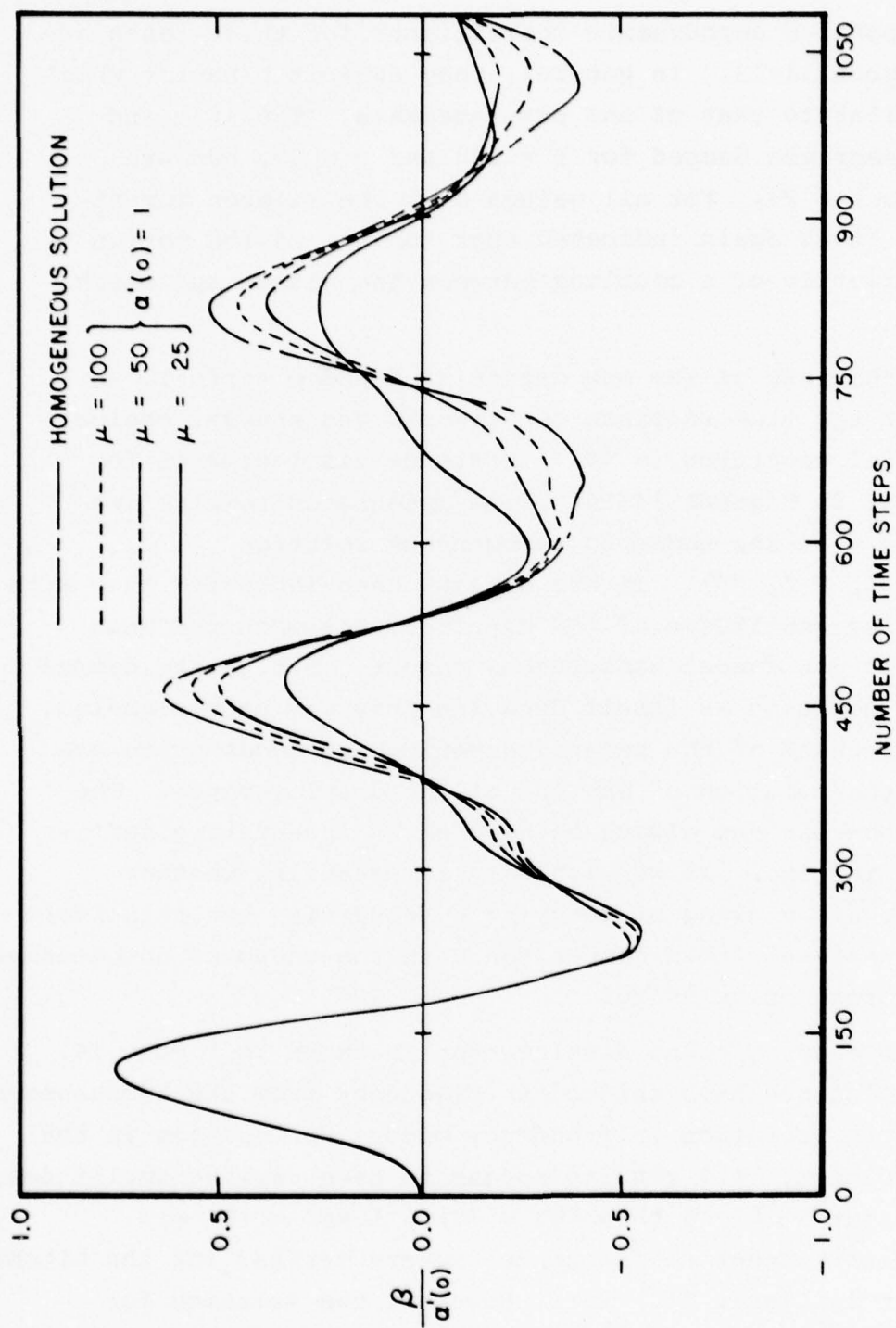


Figure 10. Unsteady Aileron Displacement for Three Degree of Freedom Airfoil with $\alpha'(0) = 1$.

Corresponding aerodynamic coefficients for these cases are found in Figure 11-13. In general, they exhibit behavior which is very similar to that of the displacements. The lift and pitching moment are damped for $\mu = 100$ and $\mu = 50$, but are growing with $\mu = 25$. For all values of μ the aileron moment is damped. It is again indicated that for $\mu = 25$ the motion consists primarily of a coupling between the plunge and pitch modes only.

As in the case of the one degree of freedom airfoil, we now consider the time response for fixed μ and several choices of the initial condition, $\alpha'(0)$. Unsteady displacements for $\mu = 25$ appear in Figures 14-16. Time integrated results are now compared with the undamped homogeneous solution (i.e., $\zeta_\sigma = \zeta_\alpha = \zeta_\beta = 0$). It has already been indicated that with $\mu = 25$ growing amplitudes of the displacements occurred when compared with the damped homogeneous result. But as the damped homogeneous solution is itself decaying this may be misleading, especially because of the several superimposed modes which are present in the solution of any one of the displacements. The long time behavior can always be deduced by integrating sufficiently far in time. If we wish only to establish whether oscillations are growing or decaying by observing the relatively small time response, then comparison with the undamped homogeneous result may prove quite useful.

The unsteady pitching displacement is shown in Figure 14. While all solutions have shifted in frequency from the homogeneous result, little variation in frequency occurs for changes in the initial condition. All results appear to have growing amplitudes, but less so for $\alpha'(0) = 5$ than for $\alpha'(0) = 1$ and $\alpha'(0) = 3$. The trend with respect to frequency is very similar for the pitching displacement in Figure 15. Here, however, the solution for $\alpha'(0) = 5$ is clearly growing whereas the other results may in fact be damped. This is also true for the aileron displacement shown in Figure 16.

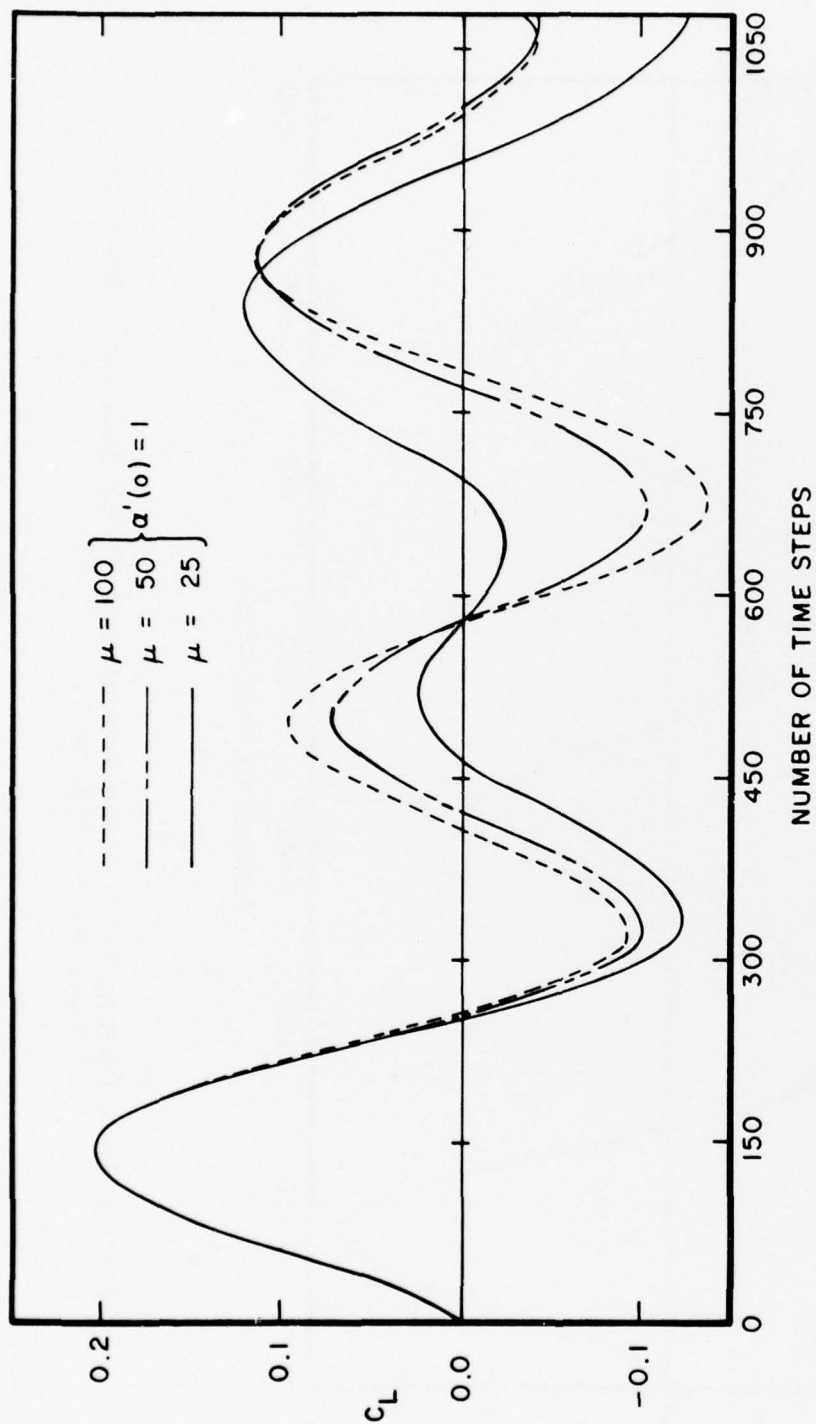


Figure 11. Unsteady Lift for Three Degree of Freedom Airfoil with $\alpha'(0) = 1$.

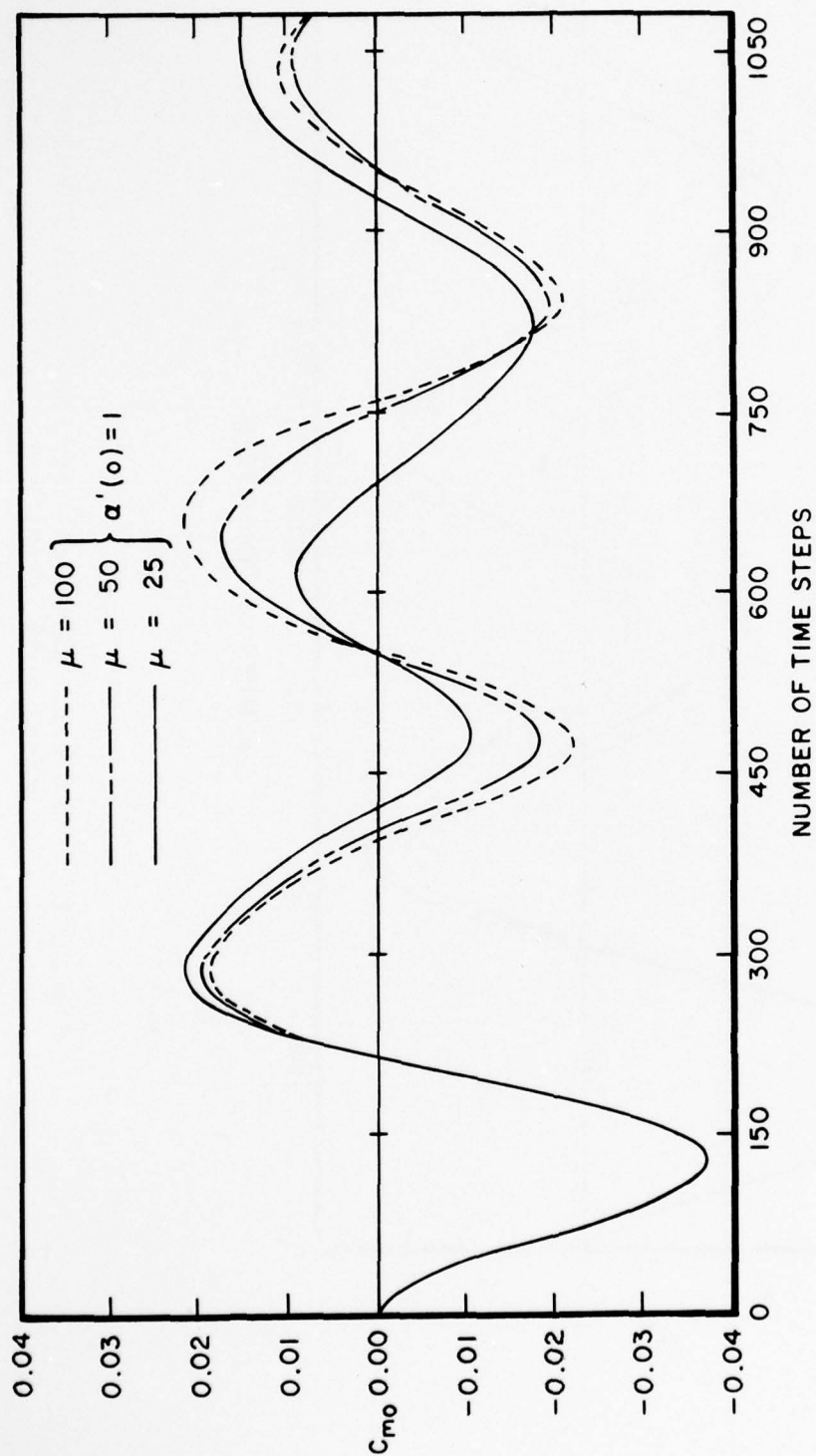


Figure 12. Unsteady Pitching Moment for Three Degree of Freedom Airfoil with $\alpha'(0) = 1$.

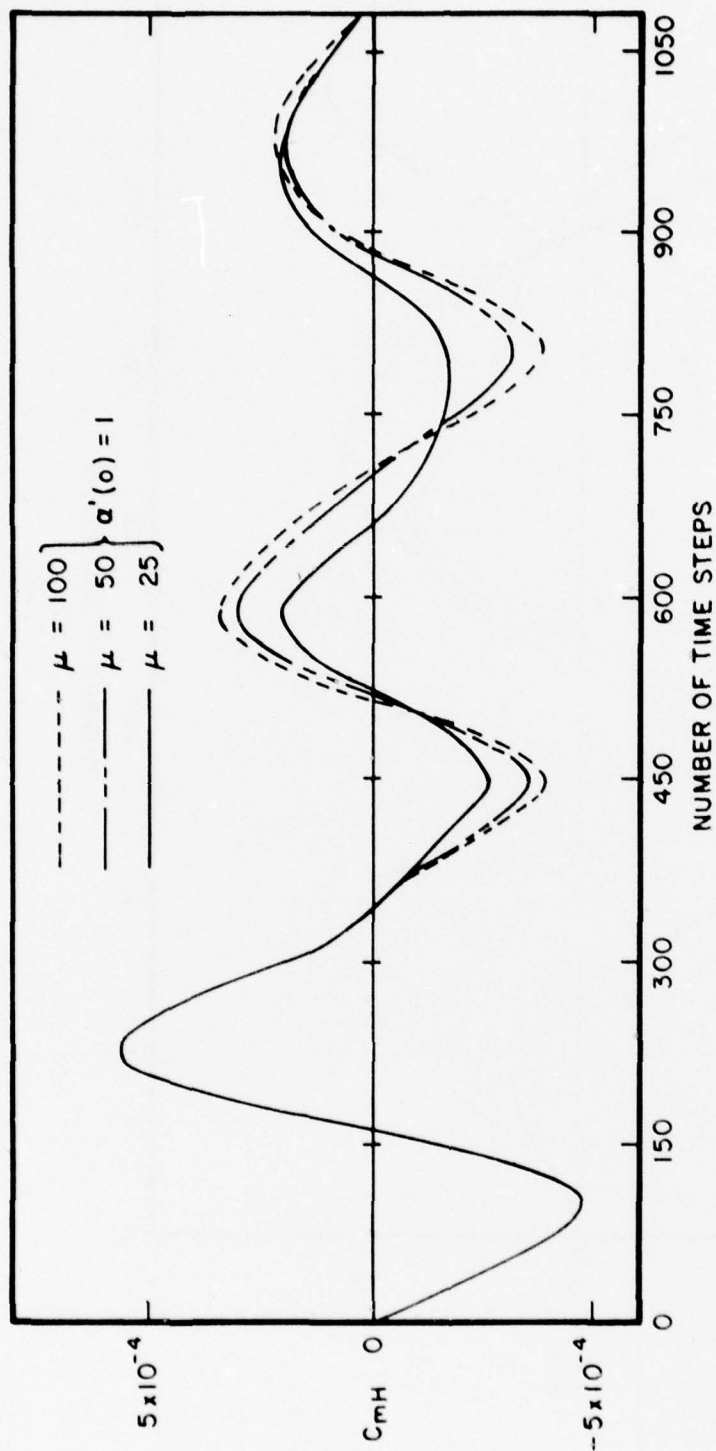


Figure 13. Unsteady Aileron Moment for Three Degree of Freedom Airfoil with $\alpha'(0) = 1$.

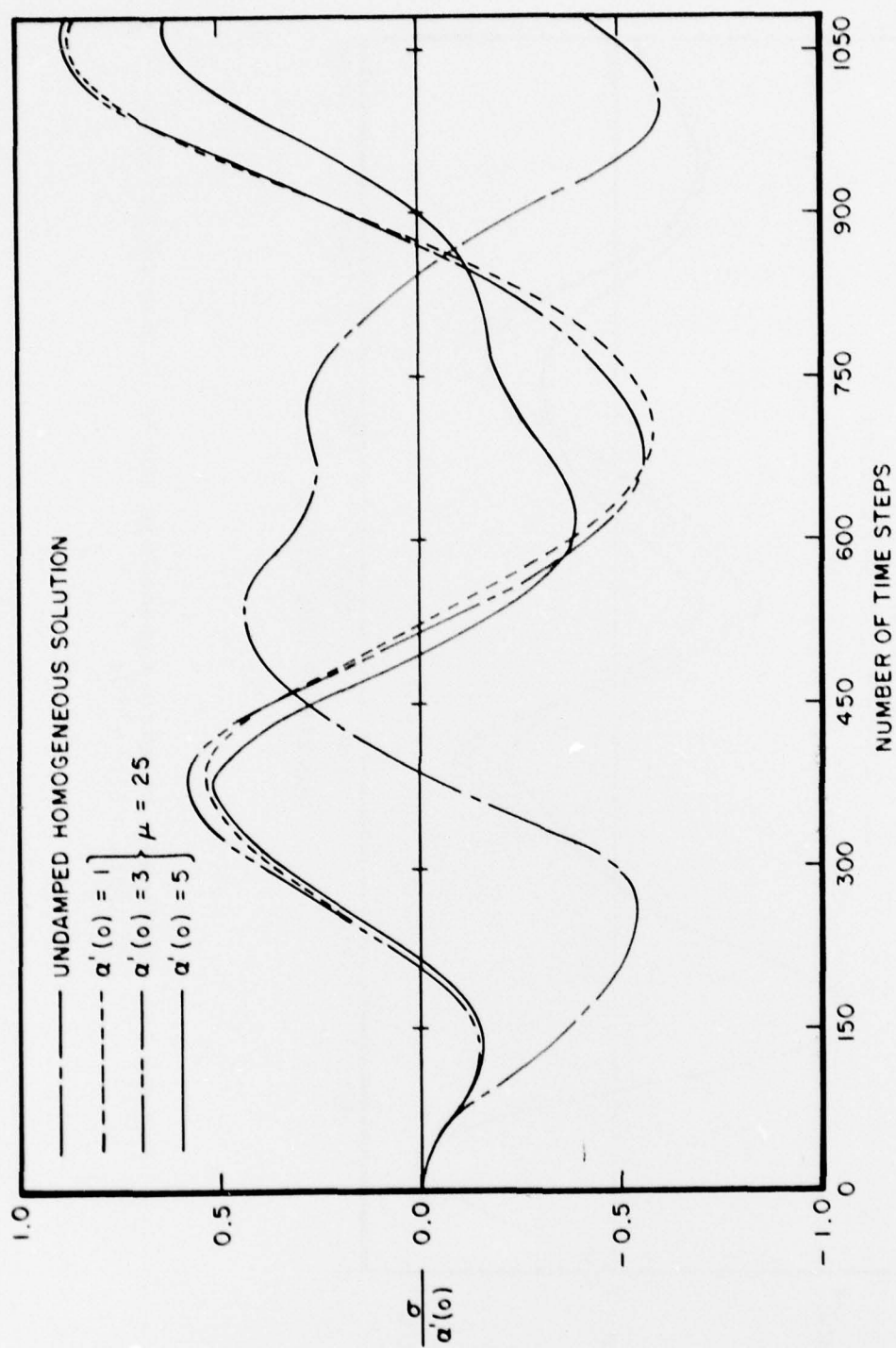


Figure 14. Unsteady Displacement for Three Degree of Freedom Airfoil with $\mu = 25$.

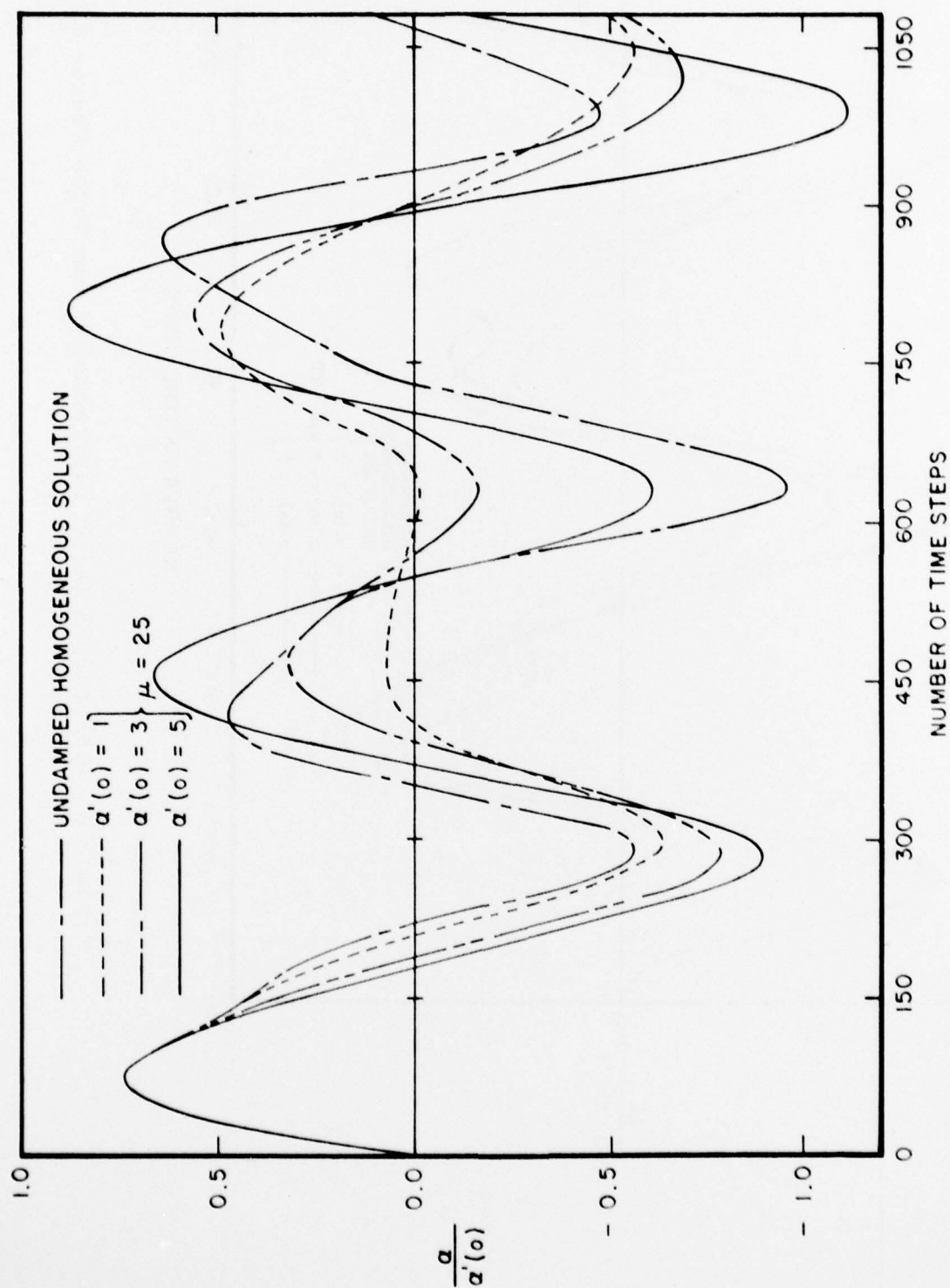


Figure 15. Unsteady Pitching Displacement for Three Degree of Freedom Airfoil with $\mu = 25$.

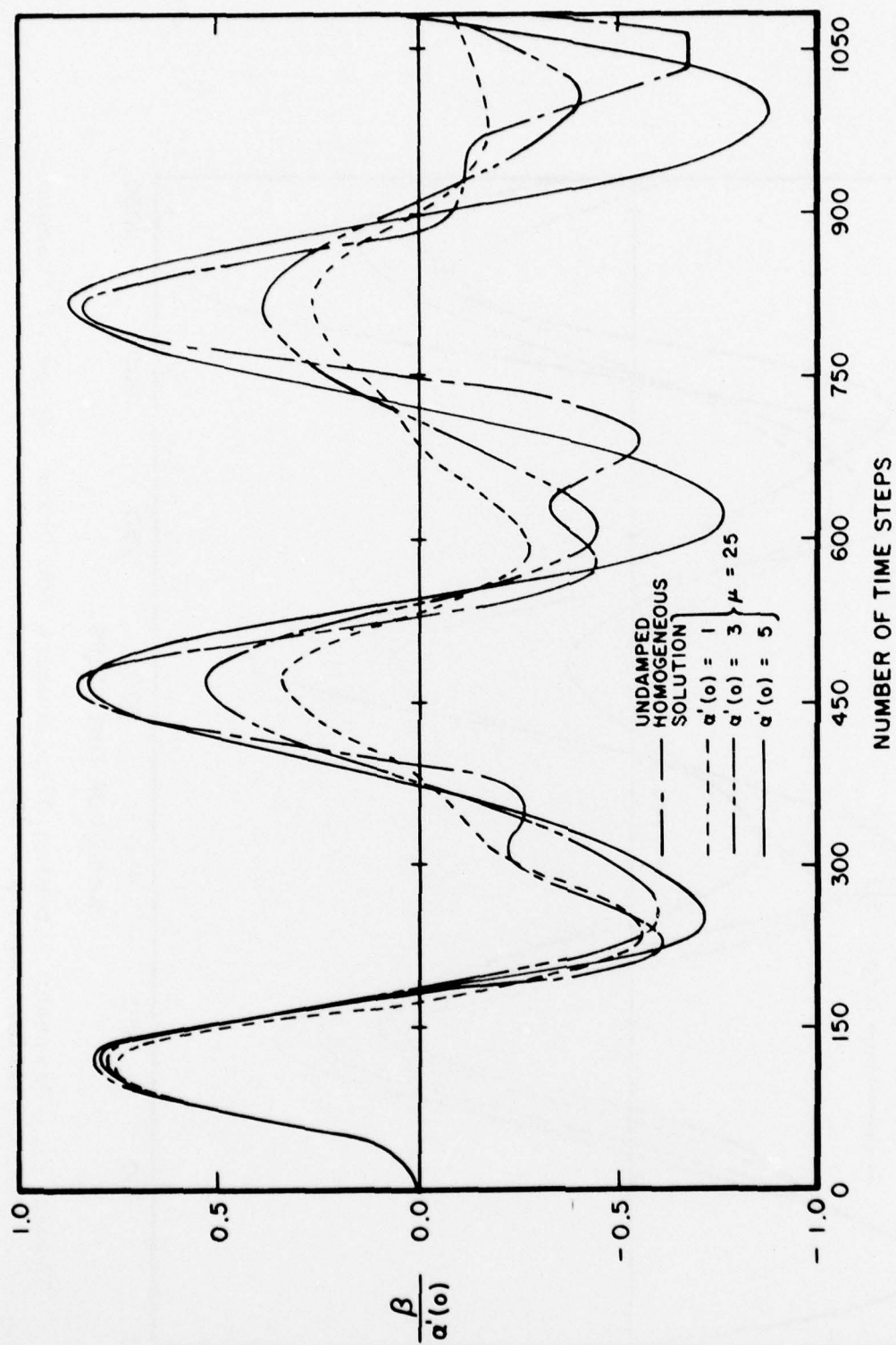


Figure 16. Unsteady Aileron Displacement for Three Degree of Freedom Airfoil with $\mu = 25$.

Figures 17-19 display the corresponding solutions for the aerodynamic coefficients with $\mu = 25$. The lift and pitching moment behavior is quite like that of the displacements. Little variation in frequency is observed for changes in the initial condition and growing amplitudes are clearly indicated for the case $\alpha'(0) = 5$. The abrupt changes in the slope of the aileron moment are due to the unsteady shock wave oscillating across the control surface. This is evident from the surface pressure distribution shown in Figure 20 for $N = 315$. The time here corresponds to relative maximums in the pitching and aileron moments and a relative minimum in the lift. For $\alpha'(0) = 5$, the entire upper surface is now subcritical while most of the lower surface has become supercritical with the shock located near the trailing edge. Recall that in the initial profile a shock was present on both surfaces near mid-chord (see Figure 3). By comparison, for the case $\alpha'(0) = 1$ the shock is displaced only slightly forward on the upper surface and slightly aft on the lower surface from its initial position. This type of shock wave motion is representative of that which can be simulated by the LTRAN2 code.

To establish the long-time behavior of the solutions, the case $\alpha'(0) = 5$ and $\mu = 25$ was integrated in time for several thousand time steps. The extended time histories of the displacements for this computation are shown in Figure 21. As was predicted from the short-time behavior, all displacements clearly exhibit increasing amplitudes. The pitching and aileron displacements are oscillating at approximately the same frequency which is about twice that of the plunging displacement. For the aerodynamic coefficients shown in Figure 22, however, all appear to have the same oscillation frequency. This extended time history indicates that such calculations may be carried out for marginally stable cases when the behavior cannot be deduced from a small-time solution. The long-time solution may in general be questionable due to the accumulation of truncation error in the time integration. Results of the forced oscillation study, however, indicate that the solutions presented here can be considered reliable.

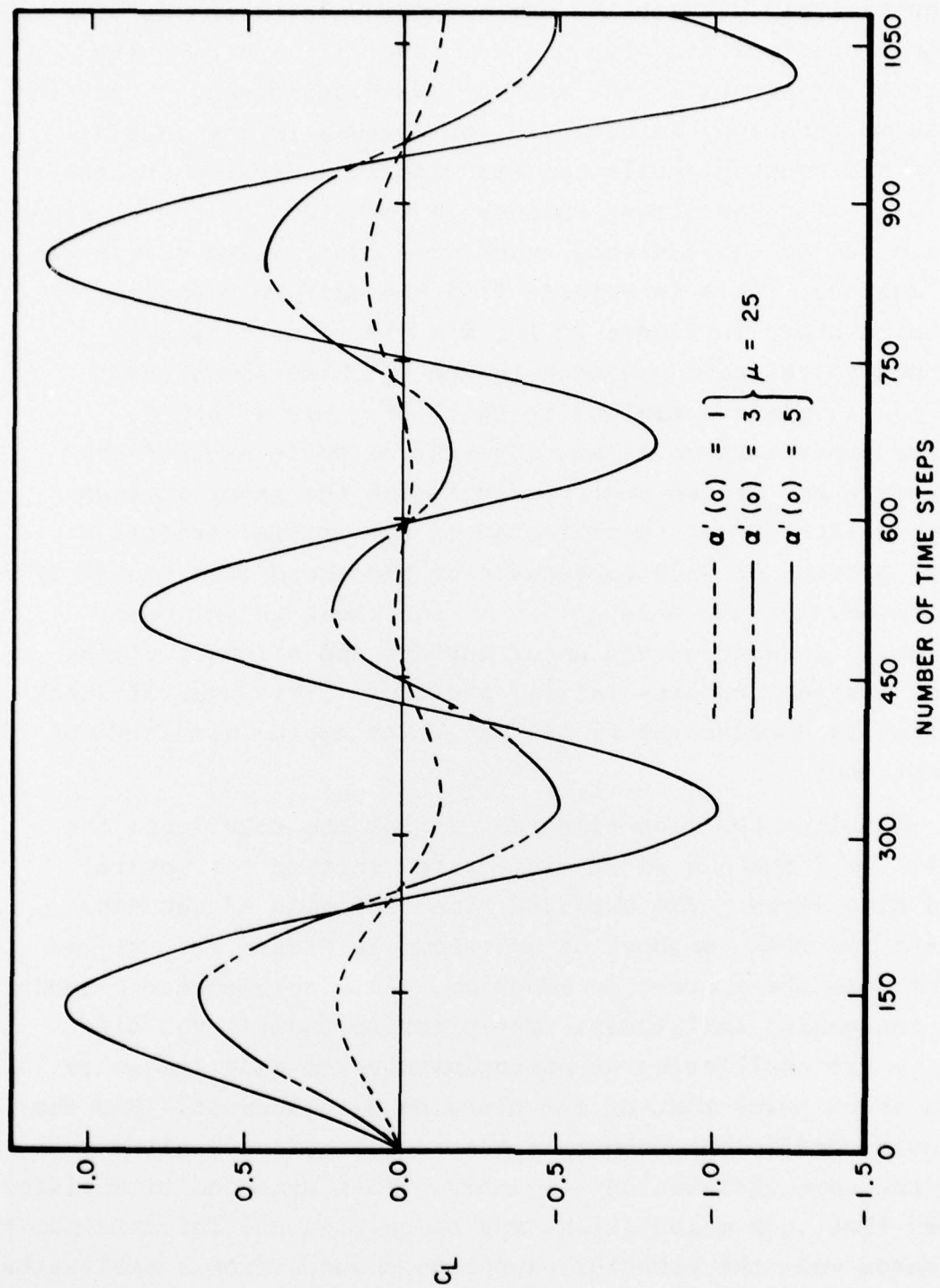


Figure 17. Unsteady Lift for Three Degree of Freedom Airfoil with $\mu = 25$.

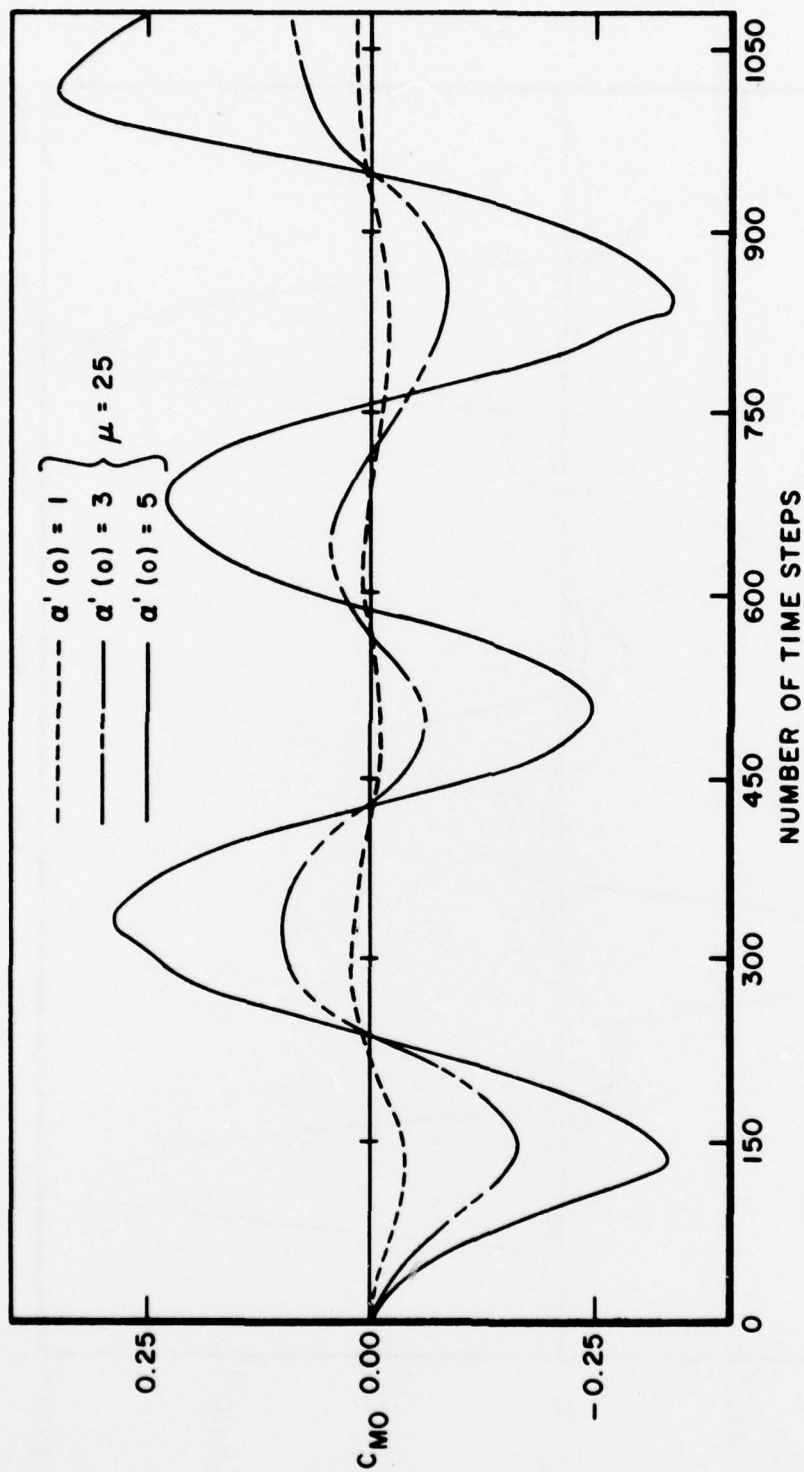


Figure 18. Unsteady Pitching Moment for Three Degree of Freedom Airfoil with $\mu = 25$.

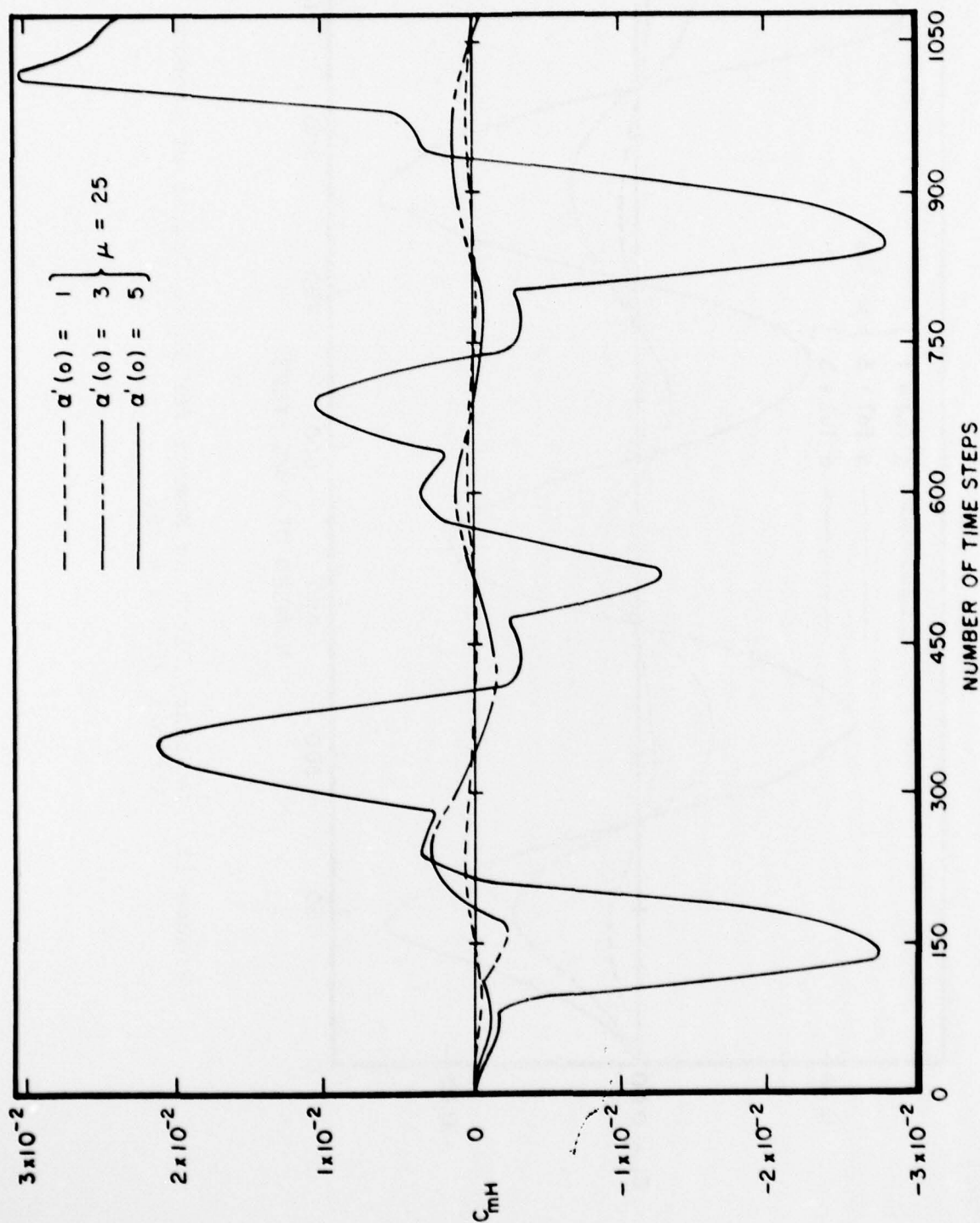


Figure 19. Unsteady Aileron Moment for Three Degree of Freedom Airfoil with $\mu = 25$.

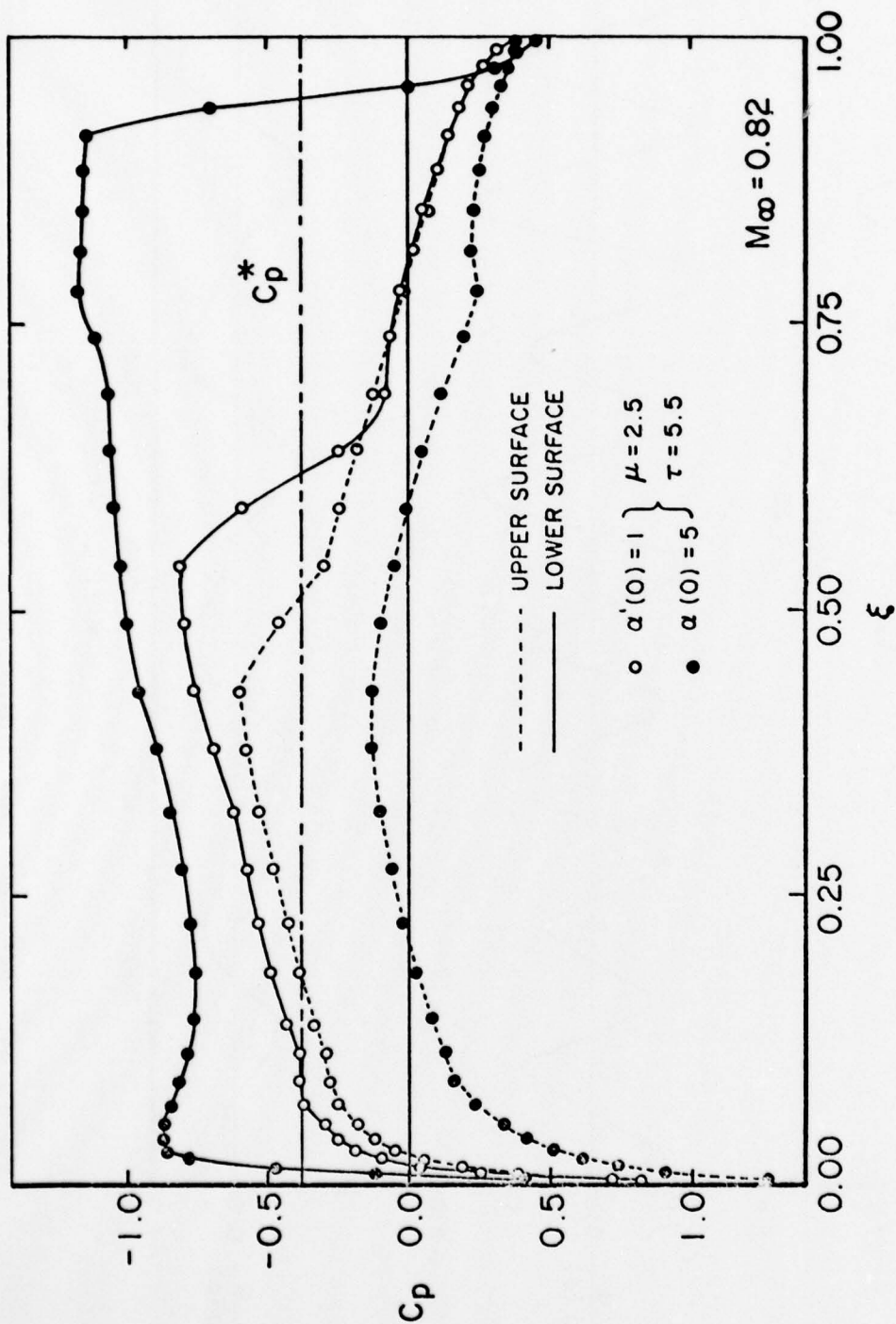


FIGURE 20. Surface Pressure Distribution for Three Degree of Freedom Airfoil with $\mu = 25$ at $N = 315$

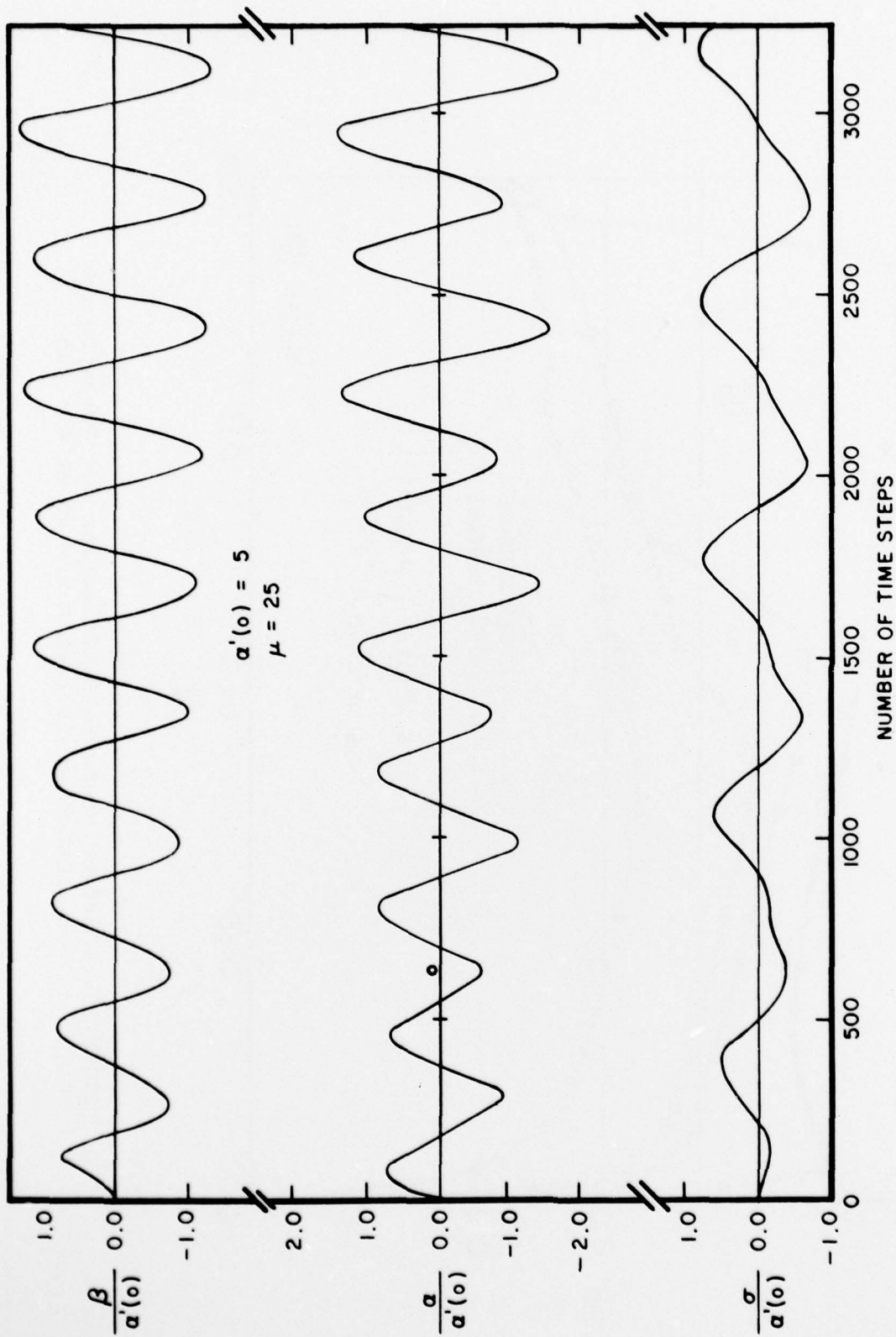


Figure 21. Extended Time History of Unsteady Displacements for Three Degree of Freedom Airfoil with $\alpha'(0) = 5$ and $\mu = 25$.

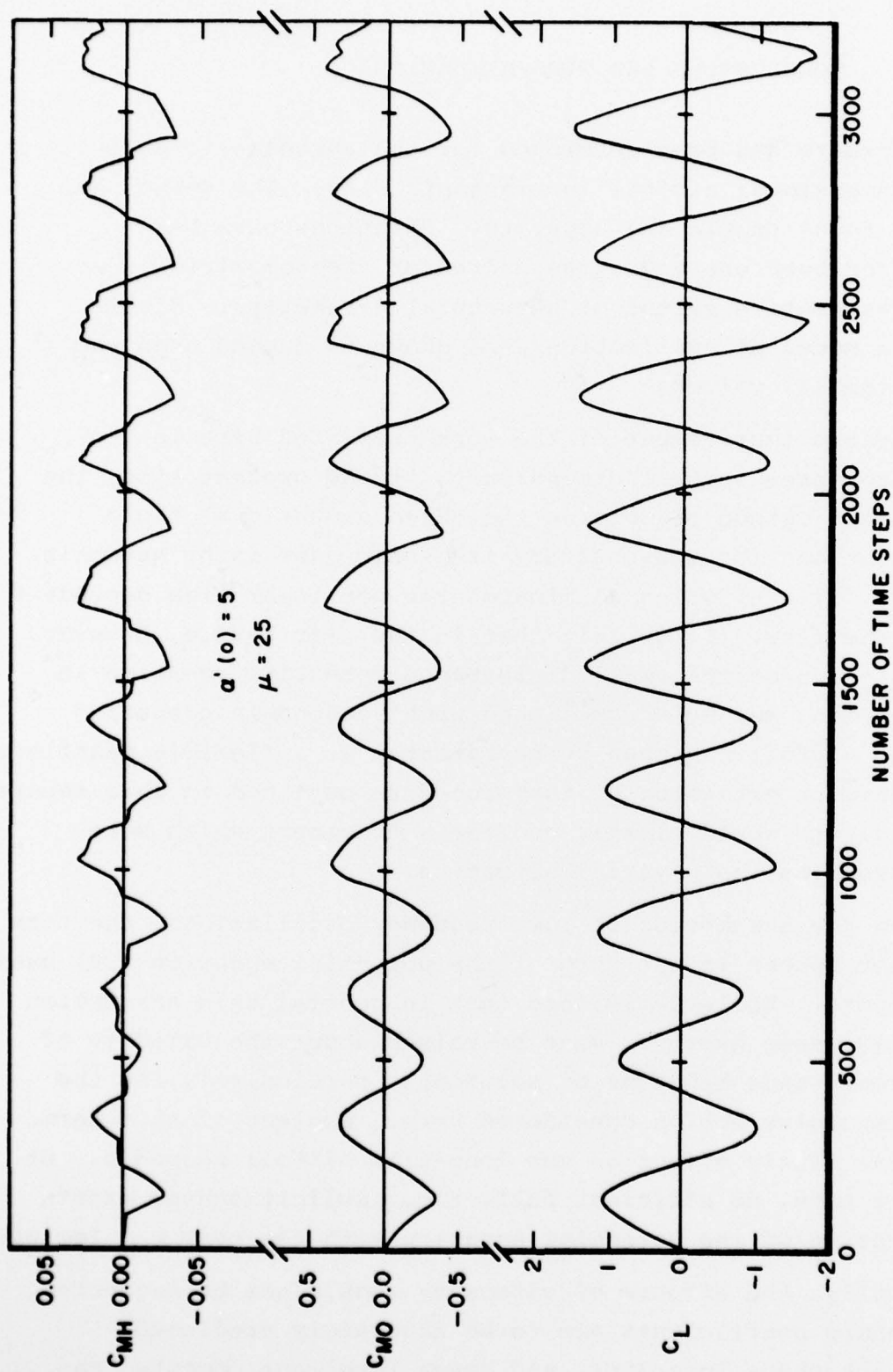


Figure 22. Extended Time History of Unsteady Aerodynamic Coefficients for Three Degree-of Freedom Airfoil with $\alpha'(0) = 5$ and $\mu = 25$.

SECTION V

CONCLUSIONS AND RECOMMENDATIONS

A procedure has been developed for the aeroelastic analysis of a two-dimensional airfoil in transonic flow. The method has been shown to be stable and accurate. Solutions have been presented for both one and three degree of freedom airfoils using representative values of structural parameters. Stable or unstable modes of oscillation were shown to depend upon the choice of initial values.

An obvious improvement of the work presented here is the extension to three spatial dimensions. At the present time, the only efficient method of solving the three dimensional fluid dynamic equations for the unsteady transonic case is by harmonic analysis (3, 5, & 6) which eliminates the nonlinear time dependent nature of the flow. It is felt that in the near future, however, time integration of the small disturbance potential equation in three-dimensions may be accomplished with reasonable computing times. The airfoil can then be represented as a flexible cantilever beam by a direct extension of the procedure outlined in this report. Such an analysis would clearly provide a treatment which more closely resembles the physical situation.

Due to the assumption of low frequency oscillations, the term ϕ_{TT} does not appear in the form of the potential equation (29) used in this report. While it is felt that in general this assumption is justified, some question must be raised about the validity of the very small-time behavior of solutions, particularly for the cases of impulsive motion considered here. Neglect of this term probably has little effect on the long-time airfoil response. At the present time, no efficient fully time implicit scheme exists for integration of the potential equation with the term ϕ_{TT} included.

Finally, the effects of viscosity should not be neglected if aerodynamic coefficients are to be accurately predicted. Instantaneous shock locations, and hence resultant moments, can

depend greatly upon unsteady viscous interaction. Coupling of the viscous effects with inviscid flow field calculations is not a simple task. In the case of unsteady transonic flows only one procedure for accomplishing this has been suggested (9), and its present application remains largely an art.

REFERENCES

1. Ballhaus, W. F., "Some Recent Progress in Transonic Flow Computations," VKI Lecture Series: Computational Fluid Dynamics, Rhode-St-Genese, Belgium, March 1976.
2. Ballhaus, W. F., Magnus, R., and Yoshihara, H., "Some Examples of Unsteady Transonic Flow," Proceedings of the Symposium on Unsteady Aerodynamics, Vol. II, pp. 769-791, 1975.
3. Ehlers, F. E., "A Finite Difference Method for the Solution of the Transonic Flow Around Harmonically Oscillating Wings," NASA CR-2257, 1974.
4. Traci, R. M., Albano, E. D., Farr, J. L., and Cheng, H. K., Small Disturbance Transonic Flows About Oscillating Airfoil, AFFDL-TR-74-37, June 1974.
5. Traci, R. M., Albano, E. D., and Farr, J. L., Small Disturbance Transonic Flows About Oscillating Airfoils and Planar Wings, AFFDL-TR-75-100, August 1975.
6. Weatherill, W. H., Sabastian, J. D., and Ehlers, F. E., "On the Computation of the Transonic Perturbation Flow Fields Around Two- and Three-Dimensional Oscillating Wing," AIAA Paper 76-99, January 1976.
7. Traci, R. M., Albano, E. D., and Farr, J. L., "Perturbation Method for Transonic Flows About Oscillating Airfoil," AIAA Journal, Vol. 14, No. 9, pp. 1258-1266, 1976.
8. Magnus, R. J. and Yoshihara, H., "Calculations of Transonic Flow Over an Oscillating Airfoil," AIAA Paper 75-98, January 1975.
9. Magnus, R. and Yoshihara, H., "The Transonic Oscillating Flap," AIAA Paper 76-327, July 1976.
10. Isogai, K., "Calculation of Unsteady Transonic Flow Over Oscillating Airfoils Using the Full Potential Equation," AIAA Paper 77-448, March 1977.
11. Beam, R. M. and Warming, R. F., "Numerical Calculations of Two-Dimensional, Unsteady Transonic Flows with Circulation," NASA TN D-7605, 1974.
12. Beam, R. M., and Ballhaus, W. F., "Numerical Integration of the Small-Disturbance Potential and Euler Equations for Unsteady Transonic Flow," NASA SP-347, Part II, pp. 789-809, 1975.

13. Ballhaus, W. F. and Steger, J. L., "Implicit Approximate-Factorization Schemes for the Low-Frequency Transonic Equation," NASA TM X-73, 082, 1975.
14. Caradonna, F. X. and Isom, M. P., "Numerical Calculation of Unsteady Transonic Potential Flow over Helicopter Rotor Blades," AIAA Journal, Vol. 14, No. 4, pp.482-488, 1976.
15. Beam, R. M., and Warming, R. F., "An Implicit Finite Difference Algorithm for Hyperbolic Systems in Conservation-Law Form," Journal of Computational Physics, Vol. 22, No. 1, pp 87-110, 1976.
16. Ballhaus, W. F. and Goorjian, P. M., "Implicit Finite Difference Computations of Unsteady Transonic Flows About Airfoils, Including the Treatment of Irregular Shock-Wave Motions," AIAA Paper 77-205, January 1977.
17. Ballhaus, W. F., and Goorjian, P. M., "Computation of Unsteady Transonic Flows by the Indicial Method," AIAA Paper 77-447, March 1977.
18. Rizzetta, D. P., Transonic Flutter Analysis of a Two-Dimensional Airfoil, AFFDL-TM-77-64-FBR, July 1977.
19. Scanlan, R. H., and Rosenbaum, R., Introduction to the Study of Aircraft Vibration and Flutter, Dover, New York, 1968, pp.192-201.
20. Isaacson, E., and Keller, H. B., Analysis of Numerical Methods, Wiley, New York, 1966, pp. 384-393.
21. Beliveau, J., "Eigenrelations in Structural Dynamics," AIAA Journal, Vol. 15, No. 7, pp 1039-1041, 1977.
22. Murman, E. M. and Cole, J. D., "Calculation of Plane Steady Transonic Flows," AIAA Paper, pp. 70-188, June 1970.